Technische Universität München

Klinik und Poliklinik für Kinder- und Jugendmedizin der Technischen Universität München, Kinderklinik München Schwabing

Mixed Lineage Leukemia 5 (MLL5) identified as disease contributing gene by single cell transcriptome analysis of classical pediatric and adult Hodgkin lymphoma

David Johann Kirchberger

Vollständiger Abdruck der von der Fakultät für Medizin der Technischen Universität München zur Erlangung des akademischen Grades eines

Doktors der Medizin

genehmigten Dissertation.

Vorsitzender: Univ.-Prof. Dr. E. J. Rummeny

Prüfer der Dissertation:

1. Univ.-Prof. Dr. St. Burdach
2. Priv.-Doz. Dr. I. Teichert von Luettichau

Die Dissertation wurde am 13.02.2014 bei der Technischen Universität München eingereicht und durch die Fakultät für Medizin am 22.10.2014 angenommen.

This work is dedicated to my parents and Sarah.

Table of Contents

List of Abbreviations

Ac	Acetylation
ACTB	Actin, beta
APS	Ammonium persulfate
7-AAD	7-Amino-actinomycin D
5-aza-dC	5-aza-deoxycytidine
BMI1	BMI1 polycomb ring finger oncogene
BRCA1	Breast cancer 1, early onset
BrdU	Bromodeoxyuridine
CD	Cluster of differentiation
CDK	Cyclin-dependent kinase
CDKN1A (p21)	Cyclin-dependent kinase inhibitor 1
cDNA	Complementary DNA
CH3	Methylation
CO_2	Carbon dioxide
CPT	Camptothecin
ddH_2O	Double-distilled water
DMSO	Dimetylsulfoxide
DNA	Deoxyribonucleic acid
DNMT	DNA methyltransferase
dNTP	Deoxyribonucleotide triphosphate
EDTA	Ethylenediaminetetraacetic acid
e.g.	exempli gratia (for example)

ELISA	Enzyme Linked Immunoabsorbent Assay
EtBr	Ethidium bromide
EZH2	Enhancer of zeste homolog 2 (Drosophila)
FACS	Fluorescence activated cell sorting
FAM	6-carboxy-fluorescein
FBS	Fetal bovine serum
FC	Fold change
FSS	Forward scatter
FSCN1	Fascin homolog 1, actin-bundling protein
GAPDH	Glyceraldehyde 3-phosphate dehydrogenase
GATA3	GATA binding protein 3
GSTM1	Glutathione S-transferase mu 1
G1P2	Interferon, alpha-inducible protein
h	Hours
HAT	Histone acetyltransferase
HCl	Hydrochloric acid
HDAC	Histon deacetylase
HL	Hodgkin lymphoma
HOX	Homeobox
HRP	Horse radish peroxidase
HRS	Hodgkin and Reed-Sternberg
HSC	Hematopoietic stem cells
H3	Histone 3
H3K4	Histone 3 lysine 4
H3K9	Histone 3 lysine 9
H3K14	Histone 3 lysine 14
H3K27	Histone 3 lysine 27
H_2O	Water

ID2	Inhibitor of DNA binding 2
IFITM1	Interferon induced transmembrane protein 1
IFN	Interferon
IL	Interleukin
JAK	Janus kinase
kDa	Kilo Dalton
KDM1A (LSD1)	Lysine (K)-specific demethylase 1A
KIF18A	Kinesin family member 18A
LT-HSC	Long-term hematopoietic stem cell
MARCKS	Myristoy- lated alanine-rich protein kinase C substrate
MBG	Minor groove binder
me2	Dimethylation
me3	Trimethylation
min	Minute(s)
MLL	Mixed lineage leukemia
mRNA	Messenger RNA
MSC (ABF1)	Musculin
MT	Methyltransferase
ncRNA	Non-coding RNA
Neg. siRNA	Non-silencing siRNA
NF-κB	Nuclear factor kappa-light-chain-enhancer of activated B cells
NFKBIA	Nuclear factor of kappa light polypeptide gene enhancer in B-cells inhibitor, alpha
NHL	Non-Hodgkin lymphoma
NTC	Non-template control
PBS	Phosphate buffered saline
PcG	Polycomb group

PCR	Polymerase chain reaction
PE	R-Phycoerythrin
PHD	Plant homeodomain
PI	Propidium iodide
POU2AF1 (BOB1)	POU class 2 associating factor 1
POU2F2 (OCT2)	POU class 2 homeobox 2
PS	Phosphatidylserin
PVDF	Polyvinylidene fluoride
qRT-PCR	Quantitative real time polymerase chain reaction
RNA	Ribonucleic acid
RNAi	RNA interference
rRNA	Ribosomal RNA
RNPC3	RNA-binding region (RNP1, RRM) containing 3
RPS27	Ribosomal protein S27
RT	Reverse transcriptase or room temperature
SDS	Sodium dodecyl sulfate
SDS-PAGE	SDS polyacrylamide gel electrophoresis
SET	Su(var)3–9, enhancer-of-zeste and trithorax
siM2	siRNA Hs_MLL5_2
siRNA	Short interfering RNA
snoRNA	Small nucleolar RNA
SOCS1	Suppressor of cytokine signaling 1
SPI1 (PU.1)	Spleen focus forming virus proviral integration oncogene spi1
SSC	Side scatter
STAT	Signal transducer and activator of transcription
TBS	Tris-Buffered Saline
TBST	Tris-Buffered Saline Tween-20

TCF3 (E2A)	Transcription factor 3
TAE	Tris base, acetic acid, EDTA
TEMED	Tetramethylethylenediamine
TNFAIP3 (A20)	Tumor necrosis factor, alpha-induced protein 3
TNFRSF8 (CD30)	Tumor necrosis factor receptor superfamily, member 8
TNFRSF17 (BCMA)	Tumor necrosis factor receptor superfamily, member 17
TP53 (p53)	Tumor protein p53
T_{Reg} cells	Regulatory T cells
TrxG	Trithorax group
TSA	Trichostatin A
WHO	World Health Organization

1 Introduction

1.1 Hodgkin lymphoma

Lymphomas are malignancies that derive from cells of the lymphatic system. According to the WHO classification of lymphoid neoplasms, they are subdivided into two large groups, non-Hodgkin lymphoma (NHL) and Hodgkin lymphoma (HL), the latter of which was first described in 1832 by Sir Thomas Hodgkin (Banerjee 2011, Campo et al. 2011). With an annual incidence of about three cases per 100,000 persons Hodgkin lymphoma is one of the most common lymphomas in the Western world, and it accounts for approximately 1% of all cancers worldwide (Diehl 2007, Küppers 2009). In industrialized countries its incidence curve typically shows a bimodal distribution with peaks at ages 15–34 years and over 60 years (Cartwright and Watkins 2004).

The WHO discriminates between two histological entities of Hodgkin lymphoma, classical HL and nodular lymphocyte predominant HL, whereat the first one mentioned is further subclassified into nodular sclerosis HL, lymphocyte-rich HL, lymphocyte-depleted HL, and mixed cellularity HL due to morphological disparities in the tumor tissue (Campo et al. 2011). The classical HL, which this work is focused on, is characterized by large specific tumor cells, the mononucleated Hodgkin cells and the multinucleated Reed-Sternberg cells, which typically stain positive for CD30 (TNFRSF8, tumor necrosis factor receptor superfamily member 8). Whereas most other tumors consist almost exclusively of malignant cells, Hodgkin and Reed-Sternberg (HRS) cells account for only about 1% of cells in the tumor. The vast majority of cells in affected lymph nodes or extralymphatic organs are benign immune cells, such as T cells, B cells, or granulocytes, which are partly attracted by the tumor cells and form an inflammatory microenvironment (Küppers 2009).

Due to a very unique immunophenotype with features of many hematopoietic cell lineages, the cellular origin of HRS cells remained uncertain for a very long time. The question was resolved when new methods, such as single-cell microdissection, were applied, and studies showed that HRS cells carried clonal rearrangements of immunoglobulin genes in the majority of cases, indicating a B cell origin. As these rearrangements showed a high number of somatic mutations in the variable domains, further evidence was provided that HRS cells might arise from germinal center B cells. Notably, these unfavorable somatic mutations that led to degradation of the B cell receptor should have caused immediate cell death, but somehow the HRS cells managed to escape apoptosis (Diehl 2007, Kanzler et al. 1996, Küppers et al. 1994, Küppers 2009). However, rare cases of HL exist where HRS cells show clonal rearrangements of the T cell receptor, demonstrating that these tumor cells might also originate from T cells in a minority of cases (Müschen et al. 2000).

After the B cell origin of HRS cells was discovered, the pathogenesis of this extraordinary disease was further evaluated. In the majority of cases HRS cells lack expression of B cell specific transcription factors, including POU2F2 (POU class 2 homeobox 2, also known as OCT2), SPI1 (spleen focus forming virus proviral integration oncogene spi1, also known as PU.1), or POU2AF1 (POU class 2 associating factor 1, also known as BOB1) and B cell surface markers, such as CD20, CD19, and CD79 (Re et al. 2001, Schwering et al. 2003). This deregulation of the B cell phenotype is partly driven by aberrant up-regulation of proteins, which inhibit pivotal B cell differentiation factors. Two of these inhibitors are MSC (musculin, also known as ABF1) and ID2 (inhibitor of DNA binding 2), which antagonize the function of TCF3 (transcription factor 3, also known as E2A), a major factor involved in B cell development (Mathas et al. 2006). Another mechanism underlying the loss of B cell specific markers is epigenetic silencing. Analyses showed that both DNA and histone methylation contribute to down-regulation of B cell genes (Seitz et al. 2011, Ushmorov et al. 2006). These same two major mechanisms, inhibition of differentiation factors and epigenetic silencing, might not only result in loss of the B cell phenotype, but they might also account for up-regulation of lineage-inappropriate gene expression, in part. Thus, HRS cells express multiple markers of other hematopoietic cell lineages, for instance T cell markers, such as CD3, CD4, and GATA binding protein 3 (GATA3), dendritic cell markers like fascin homolog 1 (FSCN1), or the epigenetic genes BMI1 polycomb ring finger onco-

gene (BMI1) and enhancer of zeste homolog 2 (EZH2) (Drexler 1992, Dukers et al. 2004, Stanelle et al. 2010). The whole complexity of this unique deregulated phenotype still remains cryptic, and probably more factors contributing to its establishment might arise in the future.

As already mentioned above, B cells acquiring unfavorable somatic mutations in the B cell receptor complex during the germinal center reaction would normally undergo apoptosis. Cellular events preventing this fate in HRS cells might therefore be crucial for Hodgkin lymphoma oncogenesis. Consequently, genetic lesions that could contribute to the survival of HRS cells were studied, and several pathways involved in proliferation and anti-apoptosis showed alterations. One of these pathways is the NF-κB pathway, a very important pathway involved in immune response, that is strictly regulated in normal cells (Ghosh et al. 1998). In HRS cells, on the contrary, the NF-κB pathway is constitutively activated through several mechanisms (Bargou et al. 1996). On the one hand, a lot of tumor necrosis factor receptors (e.g. CD40 or tumor necrosis factor receptor superfamily member 17 (TNFRSF17, also known as BCMA)) are overexpressed in HRS cells and therefore lead to constant stimulation of both the classical and alternative NF-κB signaling pathway (Carbone et al. 1995, Chiu et al. 2007). On the other hand, multiple genetic lesions have been found concerning this pathway, especially inactivating mutations of inhibitors of the pathway, such as NFKBIA (nuclear factor of kappa light polypeptide gene enhancer in B-cells inhibitor, alpha) or TNFAIP3 (tumor necrosis factor, alpha-induced protein 3, also known as A20) (Emmerich et al. 1999, Kato et al. 2009). Both mechanisms might contribute to NF-κB activity in some cases and therefore provide a proliferation stimulus for the tumor cells. Another important pathway that has been implicated in the survival of HRS cells is the JAK-STAT (janus kinase-signal transducers and activators of transcription) pathway, a central downstream mechanism for cytokine signaling (Murray 2007). Pathway activity can be augmented by autocrine and paracrine stimulation with cytokines (e.g. interleukin 6 (IL6), IL13, and IL21), or genetic lesions may lead to constitutive signaling, such as gains or amplifications of janus kinase 2 (JAK2) or inactivation of JAK-STAT inhibitory protein SOCS1 (suppressor of cytokine signaling 1) (Joos et al. 2000, Kapp et al. 1999, Lamprecht et al. 2008, Weniger et al. 2006).

Since the great majority of cells in the lymphoma tissue are non-malignant reactive cells, several studies investigated the bidirectional crosstalk between HRS cells and

bystander immune cells, such as T cells, B cells, granulocytes, or macrophages, and its role in the pathogenesis of HL. There is evidence that this interaction promotes proliferation and survival of HRS cells through receptor-ligand interaction and cytokine signaling utilizing the above-mentioned cellular pathways, on the one hand, and, on the other hand, helps tumor cells evade host immune attack by establishing an immunosuppressive milieu, mainly through attraction of regulatory T (T_{Reg}) cells (Küppers 2009, Marshall et al. 2004, Skinnider and Mak 2002, Steidl et al. 2011). Moreover, recent studies showed that an increased number of $CD68^+$ macrophages in the tumor microenvironment was associated with shortened survival of patients, therefore providing a possible new predictive marker for risk stratification (Steidl et al. 2010).

The standard therapy for classical Hodgkin lymphoma is currently a combination of multiagent polychemotherapy and involved-field radiotherapy, with overall survival rates between 80% and above 90% depending on stage of disease, in both children and adults (Evens et al. 2008, Mauz-Körholz et al. 2010). Even patients with primary progressive disease or patients in secondary relapse after first-line therapy can sufficiently be treated nowadays with hematopoietic stem cell transplantation in a lot of cases (Claviez et al. 2009). Nevertheless, these high cure rates do also have their downsides as chemotherapy and radiation may cause serious long-term toxicities including pulmonary and cardiovascular disease, infertility, and secondary cancers, such as leukemias or solid tumors, in a number of patients that cannot be ignored. Therefore, new treatment options are explored including specific antibodies, NF-κB inhibitors, or histone deacetylase inhibitors, to achieve a more targeted therapy and reduce side effects (Evens et al. 2008).

1.2 Mixed lineage leukemia 5 (MLL5)

Mixed lineage leukemia 5 (MLL5) is part of the mixed lineage leukemia (MLL) family, which consists of five members, MLL1–5 (Liu et al. 2009). They all belong to the mammalian trithorax group (TrxG) gene family, which encode for a heterogenous group of highly conserved regulatory proteins involved in development, embryogenesis, and cell proliferation. Trithorax group proteins have first been described in Drosophila

melanogaster, where they regulate the expression of homeobox (HOX) genes and other pivotal developmental genes, together with their antagonistic counterpart, the polycomb group (PcG) of proteins (Madan et al. 2009). Members of both groups are usually part of large multisubunit complexes, which function reciprocally to regulate gene expression during development through epigenetic mechanisms, such as modifications of histone tails or DNA methylation. In general, PcG proteins facilitate repressive chromatin marks, e.g. methylation of histone H3 at lysine 27 (H3K27), leading to target gene silencing, whereas TrxG proteins establish activating chromatin modifications, e.g. methylation of histone H3 at lysine 4 (H3K4), whereby chromatin gets accessible for gene transcription. Moreover, these multiprotein complexes manage to recruit further proteins, thus, TrxG complexes may recruit histone acetyltransferases (HATs), which support transcriptional activation, while PcG complexes may attract histone deacetylases (HDACs) or DNA methyltransferases (DNMTs) that favor a transcriptionally inactive state (Mills 2010). Dysregulation in the balance between these two groups, through gain or loss of function of either one of their members, may initiate or support tumor development in several tissues (Kleer et al. 2003, Leung et al. 2004, Richter et al. 2009, Ziemin-van der Poel et al. 1991).

MLL1, the human ortholog to Drosophila trithorax, is the best-characterized member of the human mixed lineage leukemia family of genes. The MLL1 gene is located at human chromosome band 11q23, and chromosomal translocations of parts of the MLL1 gene, leading to new fusion proteins with disrupted protein function, contribute to development of both lymphoid and myeloid leukemias (Ayton and Cleary 2001). Its gene product contains three PHD (plant homeodomain) zinc finger motifs, a C-terminal SET (Su(var)3–9, enhancer-of-zeste and trithorax) domain and several other domains, including three AT hooks and a methyltransferase (MT) homology domain (Jacobson and Pillus 1999). Studies showed that PHD fingers may promote protein-protein interactions via recognition and binding of histone modification, whereas the 130 amino acids large SET domain seems to be involved in methylation of lysin residues of histone proteins, especially lysin 4 of histone H3 (H3K4) in the case of MLL1 (Mellor 2006, Nakamura et al. 2002). Homozygous knockout of Mll1 ($Mll1^{-/-}$), the murine ortholog of human MLL1, results in embryonic lethality, suggesting an important role in mammalian development. Mice with heterozygous deletions of Mll1 ($Mll1^{+/-}$)

showed retarded growth, hematopoietic abnormalities, and severe transformations of the axial skeleton (Yu et al. 1995, Yu et al. 1998).

As opposed to MLL1, only little is known about the latest member of the MLL family, MLL5. The mixed lineage leukemia 5 gene is located within a segment of human chromosome band 7q22, and it was initially identified when looking for a candidate tumor suppressor gene located in this chromosome section, which is commonly deleted in myeloid malignancies (Emerling et al. 2002, Liu et al. 2009). MLL5 is expressed ubiquitous, with the highest RNA levels in fetal and hematopoietic tissues, and it encodes for a protein with 1858 amino acids and a molecular mass of approximately 200 kDa. Even though its sequence displays only little homology to those of the other MLL group members, it shares two distinct protein domain structures with them, which are characteristic for TrxG/MLL proteins, the PHD motif and the SET domain. However, unlike MLL1, it lacks both AT hooks and the MT homology domain, which are important for DNA binding, suggesting a molecular function regulated through protein to protein interactions mediated by the PHD and SET domain (Emerling et al. 2002).

In accordance with these molecular findings no direct histone methyltransferase activity was noticed on MLL5, although a global reduction of di- and trimethylated H3K4 (H3K4me2/me3) was found in mouse myoblasts after suppression of MLL5. These quantitative changes were most likely caused indirectly through regulation of other histone-modifying enzymes, such as the lysine (K)-specific demethylase 1A (KDM1A, also known as LSD1) (Madan et al. 2009, Sebastian et al. 2009). Yet, a short isoform of full-length MLL5 was identified within a multiprotein complex in undifferentiated human HL60 promyelocytic leukemia cells, which served as a mono- and dimethyltransferase to histone H3 (H3K4me1/me2) after modification with β-N-acetylglucosamine, thereby facilitating retinoic-acid-induced differentiation (Fujiki et al. 2009).

Further in vitro studies showed that MLL5 protein was strictly localized to the nucleus in a speckled manner, and that ectopically overexpression of MLL5 in HEK 293T cells (human embryonic kidney cells) induced cell cycle arrest in G_1/S phase (Deng et al. 2004). However, more recent investigations demonstrated that knockdown of MLL5 by RNA interference (RNAi) also resulted in retarded growth of both tumor and normal diploid cell lines, due to cell cycle arrest at both G_1/S and G_2/M phase.

This arrest might have been mediated by up-regulation of the cyclin-dependent kinase inhibitor 1A (CDKN1A, also known as p21) and dephosphorylation of phosphorylated retinoblastom protein (Cheng et al. 2008). Both mechanisms are well known to cause delay in cell cycle progression (Lundberg and Weinberg 1998, Waldman et al. 1995). It may seem odd that both up- and down-regulation of MLL5 may lead to cell cycle arrest, but the same controversial effect has been shown before, for example for BRCA1, suggesting a more complex role in cell cycle regulation (Deans et al. 2004, MacLachlan et al. 2000). Another study by Cheng et al. (2011) emphasizes the role of MLL5 in cell cycle control, as they showed that camptothecin (CPT)-induced down-regulation of mixed lineage leukemia 5 led to stabilization of tumor protein p53 (TP53, also known as p53), one of the most powerful tumor suppressors. It was proposed that chromatin-bound MLL5 prevents binding of p53 to the chromatin of downstream effector genes, and that degradation of MLL5 enables p53 binding to the DNA and subsequent transcription of target genes, for example CDKN1A (p21), resulting in cell cycle arrest and apoptosis. This implicates a tremendous role of MLL5 in cell cycle control and protection against apoptosis (Cheng et al. 2011).

In vivo function of murine Mll5 was investigated by three independent groups, which generated loss-of-function mutations in the murine MLL5 ortholog. Unlike homozygous Mll1 knockout mice ($Mll1^{-/-}$), homozygous inactivation of Mll5 ($Mll5^{-/-}$) did not result in embryonic lethality, even though a higher postnatal lethality was observed in knockout mice, as compared to wildtype littermates. All three groups demonstrated a critical role of Mll5 in adult hematopoiesis (Heuser et al. 2009, Madan et al. 2009, Zhang et al. 2009). Zhang et al. (2009) discovered a reduced number of long-term hematopoietic stem cells (LT-HSCs: Lin^-, Sca-1^+, c-kit^+, $CD34^-$, $FLT3^-$) in surviving animals, and an impaired capacity of LT-HSCs to reconstitute hematopoiesis in irradiated recipients, suggesting a disturbed stem cell fitness and homeostasis. Moreover, $Mll5^{-/-}$ mice showed a reduced survival after 5-fluorouracil-induced myelosuppression, indicating a disrupted regenerative potential of HSCs, which should normally quit quiescence and start dividing and differentiating to reconstitute hematopoiesis (Zhang et al. 2009). Madan and colleagues detected a reduced thymus, spleen, and lymph node size in Mll5 deficient mice, and they also demonstrated a deficiency in the hematopoietic stem/progenitor cell compartment, leading to hypersensitivity to whole-body γ irradiation (Madan et al. 2009). Last but not least, Heuser et al. (2009)

showed an increased susceptibility towards bacterial infections after Mll5 deletion, due to an impaired neutrophil function. Besides the impaired repopulation capacity of HSCs, they also illustrated that homozygous loss of Mll5 enhances sensitivity to 5-aza-deoxycytidine (5-aza-dC)-induced HSC differentiation (Heuser et al. 2009). In summary all three studies demonstrated a pivotal role of Mll5 in the regulation of the hematopoietic stem cell compartment and the development of lymphoid and myeloid lineages. Surprisingly, none of the groups detected an increased incidence of spontaneous tumors in the $Mll5^{-/-}$ mice, raising the question whether MLL5 might really act as a tumor suppressor (Heuser et al. 2009, Liu et al. 2009, Madan et al. 2009, Zhang et al. 2009).

1.3 Aim of this study

Despite the high cure rates of Hodgkin lymphoma many patients get confronted with their disease again, even decades after therapy, due to long-term toxicities caused by conventional polychemo- and radiotherapy. Therefore, our group initiated a project, including this study, to identify Hodgkin lymphoma specific gene expression and evaluate the impact of certain identified genes on the pathogenesis of HL. All of this might contribute to push the development of new tumor-specific therapy approaches with fewer adverse effects on healthy tissues.

The goal of this work was to elucidate the role of MLL5 in Hodgkin lymphoma pathogenesis. MLL5 was identified in a subset of genes from microarray analyses as overexpressed in microdissected HRS cells of pediatric and adult HL, when compared to benign $CD77^{+}$ germinal center B cells (Mollweide et al. manuscript in preparation). Based on its predicted crucial role in stem cell regulation and maturation of myeloid and lymphoid lineages, it seemed to be a promising target of research for a disease that is characterized by tumor cells with a tremendous deregulation in lineage affiliation. MLL5 messenger RNA (mRNA) expression was validated in primary tumor samples and healthy controls by quantitative Real Time PCR (qRT-PCR). Then, MLL5 was transiently knocked down by RNA interference in different HL cell lines, and phenotypical changes in proliferation and apoptosis were examined applying several in vitro assays. RNA of MLL5 knockdown and control cells was subjected to microarray

analyses in order to assess possible MLL5 downstream targets. Moreover, Western blot analyses provided an insight into a potential mechanism of MLL5 function in HL cell lines. In summary, this work focused on investigating the disease contribution of MLL5 in HL through an integrated approach, where not only the phenotype was assessed, but also underlying mechanisms were taken into account.

2 Materials

2.1 Human cell lines

All cell lines were obtained from DSMZ (German Collection of Microorganisms and Cell Cultures), Braunschweig, Germany.

Table 2.1: Description of human cell lines used in this work

Cell line	Description
L1236	Human Hodgkin lymphoma cell line, established from the peripheral blood of a 34-year-old male patient with stage IV mixed cellularity subtype.
L428	Human Hodgkin lymphoma cell line, established from the pleural effusion of a 37-year-old woman with stage IV nodular sclerosis subtype.
HDMYZ	Human Hodgkin lymphoma cell line, established from the pleural effusion of a 29-year-old patient with refractory stage III nodular sclerosis subtype.
KMH2	Human Hodgkin lymphoma cell line, established from the pleural effusion of a 37-year-old male with relapsed stage IV mixed cellularity subtype.
L540	Human Hodgkin lymphoma cell line, established from the bone marrow of a 20-year-old woman with stage IV nodular sclerosis subtype.

2.2 Media, buffers and solutions

Table 2.2: Cell culture media

Name	Ingredients
Standard medium	500 ml RPMI Medium 1640, 10% FBS, 2 mM L-glutamin, 1 mg Gentamycin

Table 2.3: Solutions and gels for Western blot analysis

Name	Ingredients
2 x Laemmli buffer	125 mM Tris-HCl, pH 6.8, 20% Glycerol, 2% SDS, 0.002% Bromphenolblue
10% APS	100 mg ammonium persulfate in 1 ml ddH_2O
4 x Seperating buffer	1.5 M Tris, pH 8.8, 0.4% SDS
4 x Stacking buffer	0.5 M Tris, pH 6.8, 0.4% SDS
Seperating Gel (12.5%)	4.17 ml 30% Acrylamide/Bis, 2.5 ml 4 x Seperating buffer, 3.33 ml ddH_2O, 50 μl 10% APS, 15 μl TEMED
Stacking Gel (4.5%)	1.05 ml 30% Acrylamide/Bis, 1.75 ml Stacking buffer, 4.2 ml ddH_2O, 100 μl 10% APS, 10.4 μl TEMED
5 x SDS Running buffer	25 mM Tris, pH 8.3, 192 mM Glycine, 0.1% SDS
5 x Transfer buffer	25 mM Tris, pH 8.3, 192 mM Glycine
10 x TBS	0.5 M Tris, pH 7.4, 1.5 M NaCl
1 x TBST (0.05%)	100 ml of 10 x TBS, 900 ml ddH_2O, 0.5 ml Tween 20

Table 2.4: Buffer and gel for RNA agarose gel electrophoresis

Name	Ingredients
50 x TAE buffer	2 M Tris, 10% EDTA (0.5 M), 5.71% HCl
1 x TAE buffer	50 x TAE buffer 1:50 (v/v) in RNase-free water
Agarose gel	200 ml 1 x TAE buffer, 0.7% agarose, 3 μl Ethidium bromide

Table 2.5: Buffers and solutions for cell cycle analysis

Name	Ingredients
Sample buffer	50 mg Glucose in 50 ml 1 x PBS, filtered through a 0.22 μm filter and stored at 4°C
20 x PI Staining solution	100 mg Propidium iodide in 100 ml H_2O, filtered through a 0.22 μm filter and stored at 4°C
1 x PI Staining solution	50 μg/ml Propidium iodide and 100 U/ml RNase A in sample buffer

2.3 General material

Table 2.6: General material

Material	Manufacturer
Cryovials	Nunc, Naperville, IL, USA
Culture dishes (Nunclon™Surface 100 mm)	Nunc, Naperville, IL, USA
Culture test plates (6- and 96-well)	TPP, Trasadingen, Switzerland
Gloves (nitrile and latex)	Sempermed, Vienna, Austria
Hybond-P PVDF membrane	GE Healthcare, Uppsala, Sweden
Parafilm	Pechiney Plastic Packaching, Menasha, WI, USA
Pipettes (5, 10 and, 25 ml)	Falcon, Oxnard, CA, USA
Pipette tips (10, 200, and 1000 μl)	MbP, San Diego, CA, USA
Pipette tips with filter (10, 200, and 1000 μl)	Biozym, Hessisch Olendorf, Germany
Safe-Lock tubes (0.5 ml and 1.5 ml)	Eppendorf, Hamburg, Germany
Syringe filters (0.2 μm and 0.45 μm)	Sartorius, Göttingen, Germany
Tissue culture flasks (75 cm^2 and 175 cm^2)	TPP, Trasadingen, Switzerland
Tissue culture flasks (75 cm^2 and 175 cm^2)	Falcon, Oxnard, CA, USA
Tubes for cell culture (15 ml and 50 ml)	Falcon, Oxnard, CA, USA
Tubes for FACS™(5 ml)	Falcon, Oxnard, CA, USA
Whatman paper	Whatman, Dassel, Germany

2.4 Chemical and biological reagents

Table 2.7: Chemical and biological reagents

Reagent	Manufacturer
Agarose	Invitrogen, Karlsruhe, Germany
Ammonium persulfate (APS)	Sigma, St. Louis, MO, USA
2-Mercaptoethanol	Sigma, St. Louis, MO, USA
BenchMark™ Prestained Protein Ladder	Invitrogen, Karlsruhe, Germany
Blue Juice Gel Loading Buffer	Invitrogen, Karlsruhe, Germany
DEPC (diethyl pyrocarbonate)	Sigma, St. Louis, MO, USA
Dimethyl sulfoxide (DMSO)	Merck, Darmstadt, Germany
Ethylenediaminetetraacetic acid (EDTA)	Merck, Darmstadt, Germany
Ethidium bromide (EtBr)	BioRad, Richmond, CA, USA
Ethanol	Merck, Darmstadt, Germany
Etoposide	Sigma, St. Louis, MO, USA
Fetal bovine serum (FBS)	Biochrom, Berlin, Germany
Gentamycin	Biochrom, Berlin, Germany
Glycerol	Merck, Darmstadt, Germany
Glycine	Merck, Darmstadt, Germany
Hydrochloric acid (HCl)	Merck, Darmstadt, Germany
HiPerFect Transfection Reagens	Qiagen, Chatsworth, CA, USA

Isopropanol	Sigma, St. Louis, MO, USA
L-glutamine	Invitrogen, Karlsruhe, Germany
Maxima™ Probe/ROX qPCR Master Mix (2 x)	Fermentas, St. Leon-Rot, Germany
Methanol	Roth, Karlsruhe, Germany
10 x Phosphate buffered saline (PBS)	Invitrogen, Karlsruhe, Germany
Polyacrylamide (30% Acrylamide/Bis)	Merck, Darmstadt, Germany
Propidium iodide (PI)	Sigma, St. Louis, MO, USA
Ready-Load 1 Kb DNA Ladder	Invitrogen, Karlsruhe, Germany
Ribonuclease A (RNase A)	Roche, Mannheim, Germany
RPMI 1640 medium	Invitrogen, Karlsruhe, Germany
Sodium dodecyl sulfate (SDS)	Sigma, St. Louis, MO, USA
Skim milk powder	Merck, Darmstadt, Germany
Sodium chloride (NaCl)	Merck, Darmstadt, Germany
Tetramethylethylenediamine (TEMED)	Sigma, St. Louis, MO, USA
Tris	Merck, Darmstadt, Germany
Trypan blue	Sigma, St. Louis, MO, USA
Trypsin/ETDA	Invitrogen, Karlsruhe, Germany
Tween 20	Sigma, St. Louis, MO, USA

2.5 Commercial reagent kits

Table 2.8: Commercial Reagent Kits

Name	Manufacturer
Amaxa®Cell Line Nucleofector®Kit L	Lonza, Basel, Switzerland
Annexin V-PE Apoptose Detection Kit I	BD Biosciences, Heidelberg, Germany
Cell proliferation ELISA BrdU Kit	Roche, Mannheim, Germany
ECL Plus™Western Blotting Detection Reagent	GE Healthcare, Uppsala, Sweden
High-Capacity cDNA Reverse Transcription Kit	Applied Biosystems, Darmstadt, Germany
RNeasy®Mini Kit	Qiagen, Chatsworth, CA, USA
TaqMan®Gene Expression Assays	Applied Biosystems, Darmstadt, Germany
MycoAlert®Mycoplasma Detection Kit	Lonza, Basel, Switzerland

2.6 Instruments and equipment

Table 2.9: Instruments and Equipment

Device	Name	Manufacturer
Balance	EW3000-2M	Kern, Balingen, Germany
Centrifuge	Multifuge 3 S-R	Heraeus, Hanau, Germany

Centrifuge	Biofuge fresco	Heraeus, Hanau, Germany
Electroporator	Amaxa®Nucleofector® I Device	Lonza, Basel, Switzerland
Electrophoresis chamber		BioRad, Richmond, CA, USA
ELISA Reader	Multiskan Ascent	Thermo Scientific, Braunschweig, Germany
Flow cytometer	FACSCalibur™	Becton Dickinson, New Jersey, NJ, USA
Freezer (−80°C)	Hera freeze	Heraeus, Hanau, Germany
Freezer (−20°C)	cool vario	Siemens, München, Germany
Freezing container	Mr. Frosti	Nalgene, Rochester, NY, USA
Fridge (4°C)	cool vario	Siemens, München, Germany
Gel documentation	Gene Genius System	Syngene,Cambridge, UK
Heating block	Thermomixer Comfort	Eppendorf, Hamburg, Germany
Hemocytometer	Neubauer	Brand, Wertheim, Germany
Ice machine	AF 100	Scotsman, Milan, Italy
Incubator	HERAcell®150	Heraeus, Hanau, Germany
Liquid nitrogen tank	L-240 K series	Taylor-Wharton, Camp Hill, PA, USA
Luminometer	Sirius Luminometer	Berthold Detection Systems, Pforzheim, Germany

Microliter syringe	710NR	Hamilton, Bonaduz, Switzerland
Micropipettes		Eppendorf, Hamburg, Germany
Microscope	AxioVert 100	Zeiss, Jena, Germany
Microscope		Leica, Wetzlar, Germany
Microwave oven		AEG, Nürnberg, Germany
Mini centrifuge	MCF-2360	LMS, Brigachtal, Germany
Multichannel pipette		Eppendorf, Hamburg, Germany
PCR cycler	iCycler	BioRad, Richmond, CA, USA
Pipetting assistent	Easypet®	Eppendorf, Hamburg, Germany
Power supplier	Standard Power Pack	Biometra, Göttingen, Germany
Real Time PCR	7300 Real-Time PCR	Applied Biosystems, Darmstadt, Germany
SDS-PAGE chamber	Minigel-Twin	Biometra, Göttingen, Germany
Semi-Dry Transfer Apparatus	Fastblot	Biometra, Göttingen, Germany
Shaker	Polymax 2040	Heidolph Instr., Schwabach, Germany
Spectrophotometer	Biowave II	Biochrom, Berlin, Germany
Sterile Bench		Heraeus, Hanau, Germany
Vortexer	Vortex-Genie 2	Scientific Industries, Bohemia, NY, USA

Water Purification System	TKA GenePure	TKA, Niederelbert, Germany
Western Blot Documentation	Gel Logic 1500 Imaging System	Carestream Health, Stuttgart, Germany

2.7 Antibodies

Table 2.10: Antibodies for Western blot analysis

Antibody	Host	Dilution	Product No.	Manufacturer
Anti-H3K4me2	rabbit	1:1000	ABE250	Millipore, Billerica, MA, USA
Anti-H3K4me3	rabbit	1:1000	17–614	Millipore, Billerica, MA, USA
Anti-H3K9/14Ac	rabbit	1:1000	06–599	Millipore, Billerica, MA, USA
Anti-Actin (I-19)	goat	1:1000	sc–1616	Santa Cruz, Heidelberg, Germany
Anti-rabbit IgG HRP	bovine	1:1000	sc–2370	Santa Cruz, Heidelberg, Germany
Anti-goat IgG HRP	bovine	1:1000	sc–2350	Santa Cruz, Heidelberg, Germany

2.8 Small interfering RNAs

Table 2.11: Small interfering RNAs

Name	Target Sequence (5'–3')	Manufacturer
Control siRNA (non-silencing)	AAT TCT CCG AAC GTG TCA CGT	Qiagen, Chatsworth, CA, USA
Hs_MLL5_2	CAG CAC TTA ATA AAT GTC CTA	Qiagen, Chatsworth, CA, USA

2.9 Primers for qRT-PCR

All TaqMan®Gene Expression Assays were obtained from Applied Biosystems, Darmstadt, Germany.

Table 2.12: TaqMan®Gene Expression Assays

Gene	Assay ID
BMI1	Hs00180411_m1
EZH2	Hs00544830_m1
GAPDH	Hs99999905_m1
GATA3	Hs00231122_m1
G1P2	Hs00192713_m1
IFITM1	Hs01652522_g1
KIF18A	Hs01015428_m1
MLL5	Hs00218773_m1

3 Methods

3.1 Processing of primary HL tumor samples and microarray analysis

Isolation of both malignant HRS cells and germinal center B cells were performed by Andreas Mollweide (Department of Pediatrics, Technical University of Munich). For isolation of single HRS cells, cryoconserved affected lymph nodes of 8 adult and 9 pediatric patients were embedded in freezing medium OCT, and 5 microns thick fresh frozen sections were prepared. Slices were then stained with hematoxylin, rinsed with DEPC water for 5 min, dehydrated in ethanol, and air-dried at room temperature (RT). Subsequently 1–30 tumor cells were microdissected with a palm laser microscope and after lysis stored at $-80°C$ until RNA preparation. Germinal center B cells, which were stained with an anti-CD77-antibody, were isolated from healthy tonsils using a micromanipulator (Mollweide et al. manuscript in preparation).

Preparation of RNA from HRS cells and benign control material as well as microarray analysis were carried out by Isabell Blochberger and Prof. Christoph Klein (Department of Pathology, University of Regensburg). Briefly, mRNA was isolated from cell lysates using microbeads targeting their 3' poly(A) tail. Then, complementary DNA (cDNA) was synthesized applying one single primer, which contains both a oligo(dT) sequence that binds the poly(A) tail and a oligo(dC) sequence at its 5' end, which is needed for further amplification of cDNA. After synthesis of the new strand a terminal transferase adds a oligo(dG) sequence to its 3' terminus. Finally, the cDNA was amplified by PCR using one single oligo(dC) primer (for additional information see Klein et al. (2002)). Amplified cDNA of 8 adult and 9 pediatric HL samples, as well as cDNA

of 12 germinal center B cells from four healthy tonsils was then subjected to microarray analyses onto Operon Human Version 4.0 OpArrays (Operon, Köln resp. Corning, Schipol-Rijk, Netherlands) according to standard protocols. Bioinformatical analysis of microarray data, including differential gene expression analyses, were performed by Matthias Maneck (Institute of Functional Genomics, University of Regensburg).

3.2 Cell culture

Hodgkin lymphoma cell lines L428, KMH2, L540 and L1236 growing in suspension and semi-adherent cell line HDMYZ were cultured in RPMI standard medium (see table 2.2) at 37°C with 5% CO_2 in a humidified atmosphere. Depending on the number of cells needed for analysis, cell lines were grown in middle-sized culture flasks (75 cm^2) containing 20 ml of medium or in large-sized culture flasks (175 cm^2) with 30 ml of medium. Saturated cultures were split 1:2 to 1:5 every 2–3 days and cells were resuspended in an appropriate volume of fresh medium. While cells growing in suspension could easily be removed from the flasks with the medium, centrifuged at 1,200 rpm for 7 min, resuspended, and spread in new culture flasks, semi-adherent HDMYZ cells had to be detached from the adherence surface. For this purpose, medium was removed, and cells were incubated for 5 min with 3 ml and 5 ml 1 x trypsin at 37°C, respectively. Dislodged cells were then centrifuged as described above, resuspended, and disseminated in new culture flasks.

For long-term storage in liquid nitrogen (−192°C) cells were resuspended at a concentration of 1 x 10^6 to 1 x 10^7 per 1 ml FBS/10% DMSO, and 1 ml aliquots of the cell suspension were transferred into prepared cryovials. For controlled freezing the vials were put into freezing boxes containing isopropanol and stored 12–24 hours at −80°C, before being moved into the liquid nitrogen freezer for further storage.

To re-culture the frozen cells, vials were removed from liquid nitrogen and thawed at room temperature until the cell suspension started to defrost. In order to remove toxic DMSO the cell suspension was transferred into a 50 ml Falcon tube carrying 5 ml of fresh standard medium, and cells were pelleted at 1200 rpm for 7 min in a centrifuge. Subsequently the pellet was resuspended in fresh medium, and the suspension was transferred into a middle-sized culture flask and cultivated in an incubator.

For most analyses cell counts had to be determined by use of a Neubauer hemocytometer. Therefore 10 μl of trypan blue was added to a small volume of cell suspension (10–40 μl), and viable cells, which excluded the stain, were counted under a light microscope.

Cell cultures were tested for affection with mycoplasma regularly using the commercial MycoAlert®Mycoplasma Detection Kit according to the manufacturer's manual. Only mycoplasma-free cell cultures were used for further analyses.

3.3 Transient RNA interference

3.3.1 Electroporation

In order to transiently reduce the amount of a specific protein, Hodgkin lymphoma cell lines L428 and L1236 were transfected with short interfering RNA (siRNA) using an Amaxa®Nucleofector®I Device. According to the optimized protocol for the L428 cell line (DSMZ), 1 x 10^6 cells were pelleted in a 15 ml Falcon tube, and the supernatant was removed completely. The cells were then resuspended in 100 μl Nucleofector®Solution (Amaxa®Cell Line Nucleofector®Kit L), 10 μl of 20 μM siRNA (see table 2.11) were added, and the solution was instantly transferred into the certified cuvette for electroporation (Program X-01). After setting the electric discharge the sample was incubated for 10 min at room temperature before being transferred into 5 ml of pre-warmed culture medium. Transfected cells were then grown for an appropriate time at humidified 37°C (5% CO_2) until further analysis. For evaluation of transient knock down efficiency RNA was isolated, and gene expression was compared to non-silencing siRNA (neg. siRNA) control by quantitative RT-PCR (see sections 3.4 and 3.6).

3.3.2 Lipofection

Semi-adherent cell line HDMYZ was transiently transfected by lipofection using HiPerFect Transfection Reagent according to the manufacturer's protocol for large-scale transfection of adherent cells in 100 mm dishes (Qiagen HiPerFect Transfection

Reagent Handbook 05/2008). 1–2 x 10^6 cells were seeded per 100 mm dish in 10 ml of culture medium and incubated under normal conditions until lipofection. For the transfection approach 3.6 μl of 20 μM siRNA (see table 2.11) were diluted in 2 ml medium without FBS, and 36 μl of HiPerFect reagent were added to the dilution. After 8 min of incubation at RT the mixture was added drop-wise onto the prepared cells. Transfected cells were then handled as described above for the suspension cell lines (see section 3.3.1).

3.4 RNA isolation

For isolation of total RNA from cultured cells the RNeasy®Mini Kit was used according to the manufacturer's protocol (Qiagen RNeasy®Mini Handbook 04/2006). Between 1 x 10^6 and 1 x 10^7 cells were spun down, lysed, and homogenized in the presence of an adequate volume of 2-mercaptoethanol-containing RLT buffer, which also inactivates RNases. To enable binding of RNA longer than 200 bases to the silica membrane of the spin columns an equal amount of 70% ethanol was added to the lysate, before the sample was applied to a RNeasy®Mini spin column and centrifuged at 10,000 rpm for 1 min. In order to reduce contamination, the membrane was consecutively washed three times with different washing buffers (1 x RW1 buffer and 2 x RPE buffer). Finally, the membrane-bound RNA was eluted in 30 μl of RNase-free water, and the concentration of RNA was determined by measuring the absorbance at 260 nm in a spectrophotometer. Isolated RNA was then either used for cDNA synthesis (see section 3.5) or stored at $-80°$C for later analyses.

3.5 cDNA synthesis

For reverse transcription (RT) of isolated RNA into single-stranded cDNA the High-Capacity cDNA Reverse Transcription Kit was used in accordance with the manufacturer's protocol (Applied Biosystems Insert P/N 4375222 REV A). Briefly, the 2 x Reverse Transcription master mix was prepared mixing 2.0 μl RT buffer, 0.8 μl dNTPs, 2.0 μl RT Random Primers, 1.0 μl MultiScribe™Reverse Transcriptase, and 4.2 μl RNase-free water. For RT reaction 10 μl of the master mix was added to an

equal volume of RNA solution (approximatly 1 μg RNA in RNase-free water), and samples were loaded into a thermal cycler, where cDNA was synthesized under the following optimized conditions: Step 1: 25°C for 10 min; Step 2: 37°C for 120 min; Step 3: 85°C for 5 min; Step 4: 4°C for ∞. Synthesized cDNA was either instantly used for examination of gene expression by quantitative Real Time PCR (see section 3.6) or stored at −20°C.

3.6 Quantitative Real Time PCR

Quantitative Real Time PCR allows quantification of mRNA levels, as the amount of inserted cDNA equates to the cellular mRNA. In this work the fluorescent reporter probe method was applied. This method allows a sequence specific quantification, as a fluorescent reporter-containing probe specifically hybridizes with its corresponding sequence inside the gene of interest, and its fluorescence can only be detected after breakdown of the probe by the exonuclease activity of the Taq polymerase that specifically amplifies the target sequence due to gene specific primers. qRT-PCR was performed by use of Maxima™Probe/ROX qPCR Master Mix (2 x) (containing the Taq DNA Polymerase, dNTPs and PCR buffer) and specific TaqMan®Gene Expression Assays (Applied Biosystems), which consist of two unlabeled PCR primers and a FAM™dye-labeled MGB probe. Analyses were performed in 96-well plates and the reaction mix was prepared according to the manufacturer's instructions (Fermentas PureExtreme™Insert) as follows: 12.5 μl Maxima™ Probe/ROX qPCR Master Mix (2 x), 1.25 μl TaqMan®Gene Expression Assays (see table 2.12), 0.5 μl cDNA template, and 10.75 μl RNase-free water. Fluorescence was detected and measured in an AB 7300 Real-Time PCR system using a three-step cycling protocol. To account for possible variation in the amount of RNA in different samples the gene expression profiles were normalized to the expression level of housekeeping gene GAPDH (glyceraldehyde-3-phosphate dehydrogenase). The mean value and standard deviation of duplicates were calculated in Microsoft Excel using the 2^{-ddCt} method.

3.7 Western blot analysis

Examination of protein expression was performed by Western blot analyses, in which proteins are separated depending on their molecular weight by gel electrophoresis, transferred onto a membrane, and afterwards identified with specific antibodies.

For this purpose whole protein lysates of cultured cells were prepared. 1–2 x 10^6 cells were pelleted, supernatant was discarded, and cells were resuspended in 50 μl of hypotonic lysis buffer (that causes cell-swelling due to osmosis) for 10 min on ice, before the 15 ml Falcon tube containing the suspension was quickly dipped into liquid nitrogen for mechanical lysis of swollen cells. Afterwards 50 μl of 2 x Laemmli buffer (containing 30 μl of 2-mercaptoethanol per 1 ml buffer) was added, and the suspension was incubated for 10 min at 70°C to denature proteins. Lysates were then homogenized using a 22 gauge needle, alliquoted, and stored at −20°C.

To separate proteins according to their size by SDS-PAGE, 12.5% polyacrylamide gels were used. After samples were boiled at 95°C for 5 min, 5-10 μl of denatured and reduced protein lysates were loaded onto the gel, and electrophoresis was performed at 100 V for 1.5–2 h. For determination of protein size a commercial prestained molecular weight marker (6–180 kDa) was utilized.

For detection by specific antibodies, proteins had to be transferred onto a membrane by applying an electrical field. Therefore, the gel and a methanol-activated PVDF membrane were sandwiched between Whatman filter papers (soaked in 1 x Transfer buffer), and transfer was done in semi-dry conditions at 2 mA/cm^2 for 2 h in a blotting device. To prevent unspecific binding of antibodies, the protein-containing membrane was blocked in 5% skim milk/TBST overnight at 4°C.

The membrane was then incubated with the primary antibody (see table 2.10), targeting the protein of interest, for 2 h at room temperature under agitation. To remove unbound antibodies the membrane was washed three times in 1 x TBST for 10 min per wash. A horseradish peroxidase (HRP)-conjugated secondary antibody was then added to the membrane for another 1–2 h, and the membrane was thereupon washed again three times in 1 x TBST and once in 1 x TBS for 10 min per wash. All antibodies were diluted in 5% skim milk/TBST at recommended dilutions.

Visualization of protein-antibody complexes was achieved using the ECL Plus™Western Blotting Detection Reagent according to the manufacturer's instructions (GE Healthcare Booklet RPN2132PL Rev D 2006). This reagent generates a chemifluorescence signal in the presence of the antibody-coupled HRP and peroxide, which was detected by a CCD imaging system (Kodak Gel Logic 1500 Imaging System). After analysis of images with the provided software (Kodak Molecular Imaging Software, Version 5.0) the membrane was washed once in 1 x TBS for 15 min and then dried. Images were finally arranged using Adobe Fireworks CS4 and Microsoft PowerPoint.

3.8 Proliferation Assay (BrdU Incorporation Assay)

Proliferation of cultured cells was assessed using Cell Proliferation ELISA, BrdU Kit according to the manufacturer's instructions (Roche Manual 08/2007). 1 x 10^6 cells were transiently transfected (see section 3.3) and incubated for 1 h at humidified 37°C (5% CO_2) in an incubator. After dilution, 1 x 10^5 cells per well were seeded in a 96-well plate (flat-bottomed for semi-adherent HDMYZ and round-bottomed for L428 and L1236) in hexaplicates at a total volume of 200 μl and cultured as mentioned above. Subsequently, 20 μl/well of BrdU (5-bromo-2'-deoxyuridine) labeling solution was added to the cells at specific time points (5 h, 29h, 53 h and 77h after transfection), and cells were reincubated for another 17 h in the presence of BrdU, which gets incorporated in the DNA of proliferating cells. Labeling medium of semi-adherent HDMYZ was then removed by aspiration, while suspension cells had to be centrifuged at 300 g for 10 min, before medium could be aspirated with a multichannel pipette. Cells were then dried with a hair dryer for 15 min and stored at 4°C until analysis within the next 1–4 days. For analysis cells were fixed and lysed, before being incubated with a peroxidase conjugated anti-BrdU-antibody, which specifically binds to BrdU incorporated in the cellular DNA. After a washing step the substrate solution was added to the cells, and absorbance of the reaction product was measured at 450 nm in an ELISA reader. To exclude unspecific binding of the antibody each experimental approach had a background control with cells only, and medium with and without

BrdU. The mean value and standard error of the mean of hexaplicates were calculated and displayed using Microsoft Excel.

3.9 Apoptosis Assay

To examine apoptosis of cultured cells the Annexin V-PE Apoptosis Detection Kit I was used following the manufacturer's instructions (BD Pharmingen™ Technical Data sheet rev. 006 2004). Annexin V is a phospholipid-binding protein with a high affinity to phosphatidylserin (PS), a membrane protein that gets exclusively exposed to the outer leaflet of the plasma membrane during early stages of apoptosis. To differentiate between viable cells with an intact plasma membrane and nonviable cells that lost membrane integrity 7-Amino-Actinomycin D (7-AAD) was used. Combination of these two markers allowed discrimination between viable cells (Annexin V-PE and 7-AAD negative), early apoptosis (Annexin V-PE positive, 7-AAD negative), and end stage apoptosis (Annexin V-PE and 7-AAD positive).

For analysis cells were counted, washed twice with PBS, and 1 x 10^5 cells, suspended in 100 μl of 1 x binding buffer, were stained with 2 μl of Annexin V-PE and 7-AAD. After 15 min of incubation at RT another 400 μl of 1 x binding buffer were added, and samples were analyzed by flow cytometry using a FACSCalibur™ Flow cytometer. For each of the examined cell lines FSC, SSC and the correct parameters for detection of fluorescence were determined using unstained and single stained samples. Results were calculated and visualized using Microsoft Excel.

3.10 Cell Cycle analysis

Analysis of cell cycle was conducted by flow cytometry after staining of nuclear DNA with propidium iodide (PI). PI intercalates into double-stranded nucleic acids and emits a fluorescence signal after excitation by a 488 nm laser. The strength of the emitted signal corresponds with the cellular DNA content and therefore allows distinguishing between different phases of the cell cycle. Cells in the G_0/G_1 phase show the lowest amount of DNA with only one chromatid per chromosome, but DNA content

increases during S phase when the cellular DNA is duplicated, and reaches its highest level in G_2/M phase where the amount of DNA, and thus the fluorescence signal, is twice as high as it was in G_0/G_1 phase.

5 x 10^5 cells were washed with pre-cooled probe buffer three times and afterwards centrifuged at 1,200 rpm for 10 min (4°C). Supernatant was discarded completely, and 1 ml ice-cold 70% ethanol was added to the pellet drop-by-drop while constantly vortexing. Samples were fixed in the ethanol overnight at 4°C. The next day cells were centrifuged at 1,500 rpm for 15 min, and ethanol was poured off, before samples were resuspended in 1 ml of PI staining solution (containing 100 U/ml RNase A). Following, samples were incubated at 25°C for 45 min under agitation, for RNase A to degrade double-stranded RNA, and PI to bind to the cellular DNA. Finally, analysis was performed using a FACSCalibur™ Flow cytometer and results were displayed graphically using Microsoft Excel.

3.11 Microarray analysis

To examine changes in cellular gene expression in consequence of siRNA mediated transient protein knock down (see section 3.3) microarray analyses were performed. For this purpose total RNA of control cells and knock down cells was gathered (see section 3.4) 60 h after transfection, and knock down efficiency was examined by qRT-PCR (see section 3.6). To rule out unspecific effects due to induction of an interferon (IFN) response after transfection, mRNA levels of IFN responsive genes G1P2 (interferon, alpha-inducible protein) and IFITM1 (interferon induced transmembrane protein 1) were monitored by qRT-PCR, and only samples with an induction below twofold were used for microarray analyses.

To further exclude contamination of RNA, purity was measured spectrophotometrically, and only samples with a ratio of the absorbance at 260 and 280 nm ($A_{260/280}$) around 2 were used for further analyses. RNA integrity was assessed by 0.7% agarose gel electrophoresis where two distinct 28S and 18S ribosomal RNA (rRNA) peaks had to be seen.

Total RNA was processed and hybridized on Affymetrix GeneChip®Human Gene 1.0 ST Arrays according to standard protocols (for further information visit www.affymetrix.com) by the Affymetrix Expression Core Facility at the Department of Microbiology (Technical University of Munich). Expression data was analyzed and graphically displayed using Microsoft Excel. For creation of heat maps of the top 60 up- and down-regulated genes, signal intensities were $\log_2$ transformed and median-centered by use of the Genesis software (Release 1.7.6.) (Sturn et al. 2002). Finally some genes of interest were validated using qRT-PCR (see section 3.6).

3.12 Statistical analysis of data

All p-values were determined by conventional two-sided t-test using Microsoft Excel, if not mentioned otherwise.

For evaluation of expression data of MLL5 in primary Hodgkin lymphoma and germinal center B cells, $\log_2$ transformed median-centered signal intensities of microarray analysis were displayed as a scatter dot plot using GraphPad Prism version 5.0b for Mac OS.

To determine significance of overlap between MLL5-downregulated genes and genes that were higher expressed in chemoresistant L1236 as compared to chemosensitive L540, Fisher's Exact Test was used, according to the following 2x2 contingency table.

Table 3.1: Contingency table for Fisher's Exact Test according to Fury et al. (2006)

	col1	col2	total
row1	m	$n_1 - m$	n_1
row2	$n_2 - m$	$n - n_1 - n_2 + m$	$n - n_1$
total	n_2	$n - n_2$	n

N is the total number of genes on the Affymetrix GeneChip®Human Gene 1.0 ST Array (28,869 genes), n_1 the number of genes down-regulated after MLL5 knock down (11,336 genes), n_2 the number of genes with an higher expression in chemoresistent L1236 (43 genes), as described in (Staege et al. 2008), and m the number of overlapping genes between the two populations.

4 Results

4.1 MLL5 is overexpressed in primary HL samples as compared to germinal center B cells

As most of the genes involved in HL pathogenesis were mainly identified in HL cell lines and only partially verified in primary tumor samples, we intended to analyze gene expression profiles of primary tumor cells. Therefore, HRS cells of 9 pediatric and 8 adult HL patients were isolated from affected lymph nodes using single cell laser microdissection and compared to $CD77^+$ germinal center B cells from healthy tonsils (see section 3.1). Microarray analyses of total cellular RNA revealed several differentially expressed genes. MLL5 was one of the genes that showed a higher expression in primary HRS cells than in healthy control samples (see figure 4.1).

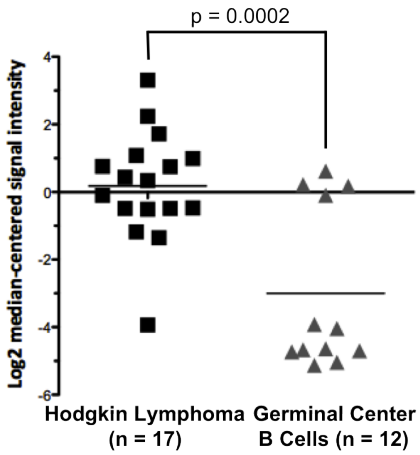

Figure 4.1: Microarray data of MLL5 expression in tumor and control samples. Scatter dot plot with the signal intensities from the MLL5 reporter on the Operon Human Version 4.0 OpArray. Plots represent data of $\log_2$ transformed median-centered signal intensities of 12 germinal center B cells and 17 HL samples from 8 adult and 9 pediatric patients, respectively.

In order to validate the observed overexpression in microarray analyses, MLL5 mRNA levels were quantified in a random selection of both primary tumor samples and control samples (see figure 4.2). qRT-PCR analyses using a specific MLL5 gene expression assay detected a high expression of MLL5 in all tumor samples reviewed, with highest mRNA levels in pediatric samples, whereas no MLL5 transcripts could be amplified in the control samples. Furthermore, qRT-PCR confirmed a broad variation in the expression of MLL5 in the tumor samples, which was already seen in the microarray analyses.

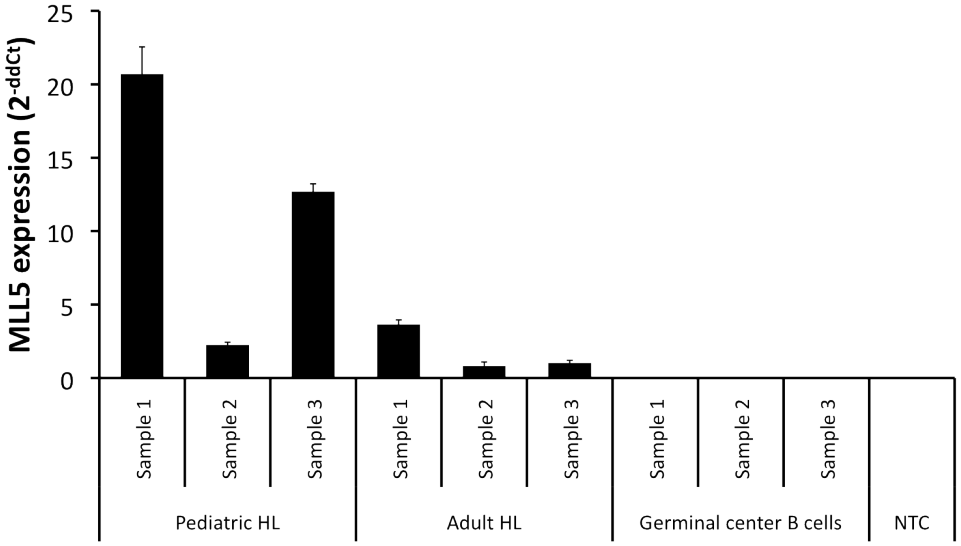

Figure 4.2: qRT-PCR verification of MLL5 expression in tumor and control samples. Expression of MLL5 on mRNA level in three pediatric and adult HL tumor samples as well as in three germinal center B cell samples quantified by qRT-PCR is shown. NTC, non-template control (H_2O).

4.2 RNA interference using siRNA leads to reduced MLL5 mRNA levels in HL cell lines

After MLL5 overexpression was shown in primary tumor samples in both microarray and qRT-PCR analyses, the effect of high cellular MLL5 expression had to be investigated in HL cell lines. First of all, qRT-PCR analyses were performed to assess the MLL5 expression in several HL cell lines, in order to identify a subset of cell lines for

further in vitro assays. Figure 4.3 shows the five HL cell lines evaluated for MLL5 expression, four of them with a B cell background (L428, L1236, HDMYZ and KMH2) and one with a T cell background (L540). Highest MLL5 mRNA levels were found in L428 and L540, whereas expression was comparable in the other three cell lines. In consideration of biological background, growing conditions, and MLL5 expression, L428, L1236, and HDMYZ were selected for further investigations.

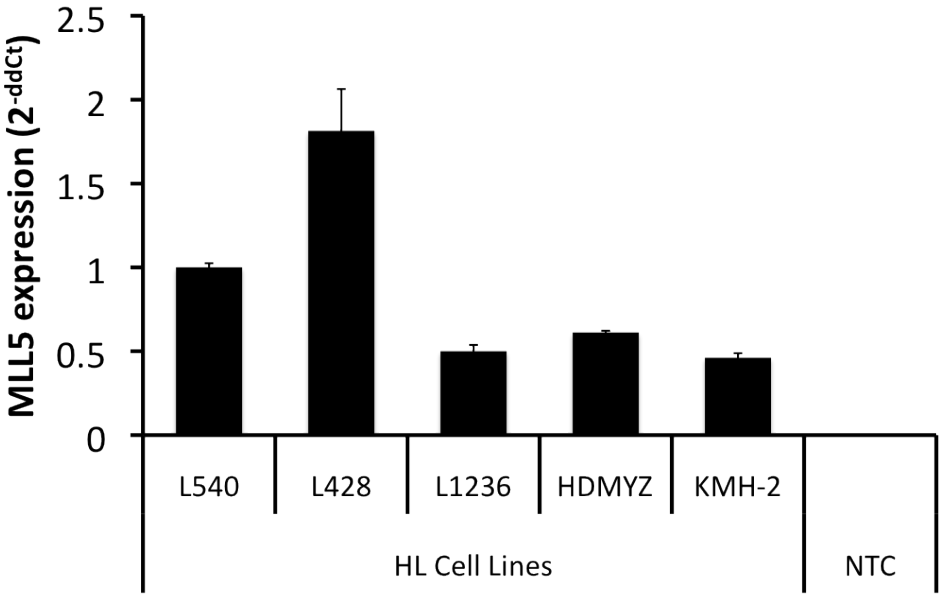

Figure 4.3: Quantification of MLL5 mRNA levels in HL cell lines by qRT-PCR. MLL5 mRNA expression was assessed in several HL cell lines (L540, L428, L1236, HDMYZ and KMH2). NTC, non-template control (H_2O).

MLL5 was then transiently knocked down by siRNA mediated RNAi in these three cell lines, as described in section 3.3 (for siRNA target sequences see table 2.11). 48–94 hours after transfection, RNA was isolated, and MLL5 gene expression in cells treated with either Hs_MLL5_2 siRNA (siM2) or non-silencing siRNA (neg. siRNA) was evaluated by qRT-PCR. Figure 4.4 illustrates knockdown of MLL5 in three different cell lines at three distinct moments, 48h, 60h, and 70h or 94h after transfection. As shown, siM2 mediated RNAi resulted in a MLL5 down-regulation to 20–40% of the value in control cells after 48h. Moreover, knockdown efficiency was still sufficient for up to 70h or 94h after transfection, with mRNA levels around 30% of the value in control cells for HDMYZ and 50–60% of the value in controls for L428 and L1236.

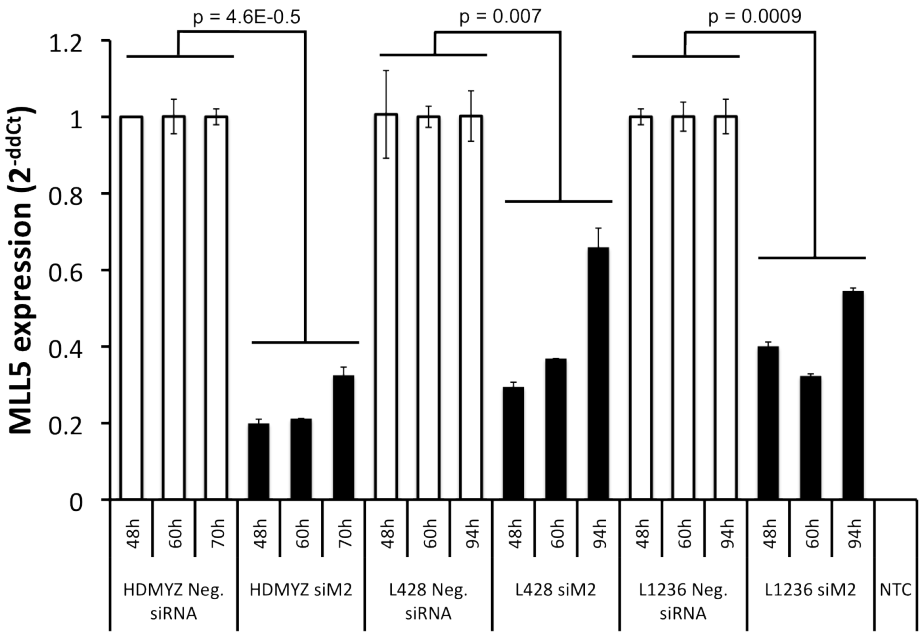

Figure 4.4: qRT-PCR analyses of MLL5 mRNA levels 48–94h after siRNA mediated RNAi. MLL5 mRNA expression is shown in three HL cell lines (HDMYZ, L428 and L1236) treated with either specific MLL5 targeting siRNA (siM2) or neg. siRNA. Analyses were performed 48h, 60h, 70h or 94h after transient transfection. NTC, non-template control (H_2O).

4.3 MLL5 down-regulation inhibits proliferation

As MLL5 was already described to promote cellular growth (see section 1.2), proliferation of HL cell lines after MLL5 down-regulation was analyzed by BrdU incorporation assays (see section 3.8). In order to obtain a growth curve of all three HL cell lines, BrdU incorporation of siRNA treated cells, which is proportional to cell proliferation, was measured 5–22h, 29–46h, 53–70h, and 77–94h after transient transfection. Figure 4.5 shows these graphs for HDMYZ, L428 and L1236. The light gray lines indicate growth of neg. siRNA treated cells and the black lines show proliferation of MLL5 knockdown cells in one experiment. As can be seen from this graphs, all three cell lines showed a reduced proliferation after knockdown of mixed lineage leukemia 5. At each reading point RNA of knockdown and control cells was isolated to monitor MLL5 down-regulation. Sufficient knockdown efficiency was observed at all time (see figure 4.4).

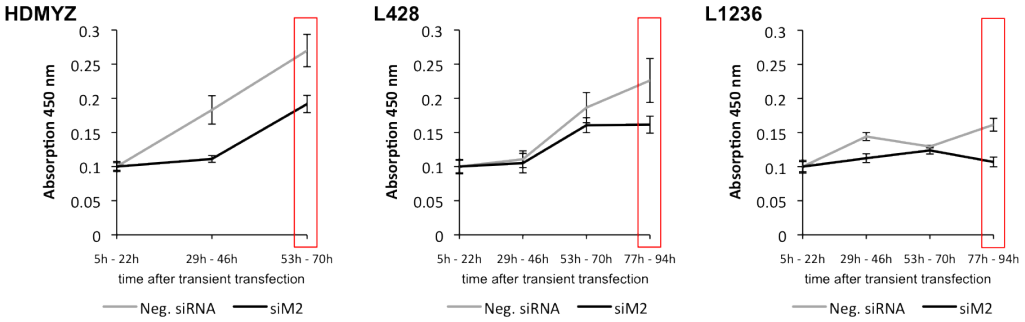

Figure 4.5: BrdU incorporation assays of HL cell lines treated with either neg. siRNA or siM2. Transiently transfected cells were incubated with BrdU for 17h after different incubation periods, before absorption at 450 nm was measured. Error bars indicate standard error of the mean of hexaplicates/group.

To further validate these results, proliferation was measured two more times in the indicated periods (red boxes). The combined results of all three independent experiments per cell line are shown in figure 4.6. A highly significant reduction in proliferation of about 40% after knockdown of MLL5 could be observed in all HL cell lines tested as compared to proliferation of cells treated with neg. siRNA.

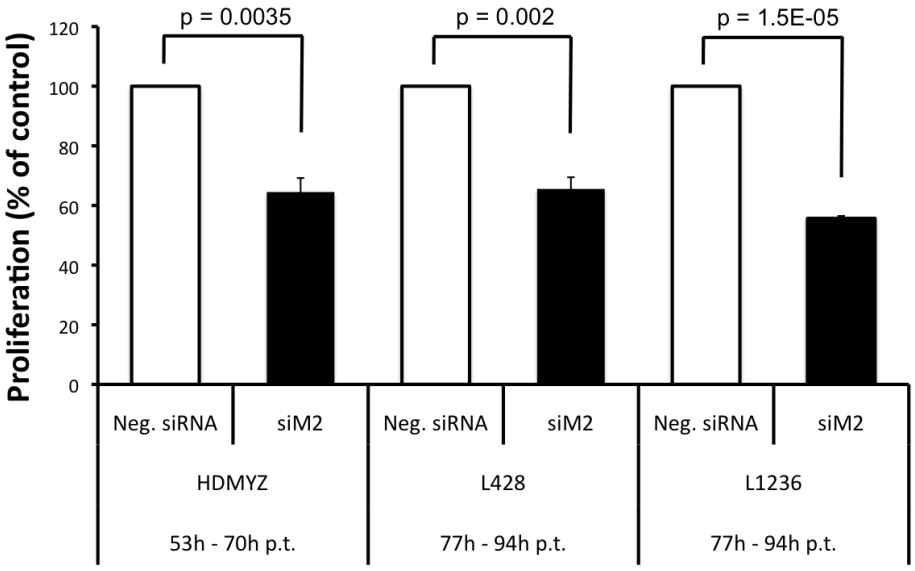

Figure 4.6: Summary of BrdU incorporation assays of HL cell lines 70h or 94h after treatment with either neg. siRNA or siM2. Data is mean and standard error of the mean of three independent BrdU incorporation assays per HL cell line. P.t., post transfectionem.

4.4 MLL5 down-regulation does not increase spontaneous apoptosis

To analyze whether MLL5 down-regulation influences cell viability in HL cell lines, apoptosis was examined using the Annexin V-PE Apoptosis Detection Kit I (see section 3.9). Cells were transiently transfected with siRNAs and incubated for 48h in a humidified atmosphere, before apoptosis was determined by FACS analyses. As shown in figure 4.7 no significantly increased apoptosis could be detected in any HL cell line tested. Quite the contrary, HDMYZ and L428 showed a 10–25% lower apoptosis rate in MLL5 knockdown cells as compared to control cells. Yet, this difference was only statistically significant for cell line L428. These results suggest that the reduced proliferation observed in these cell lines was rather caused by other factors, such as changes in cell cycle, than by increased apoptosis in MLL5 knockdown cells.

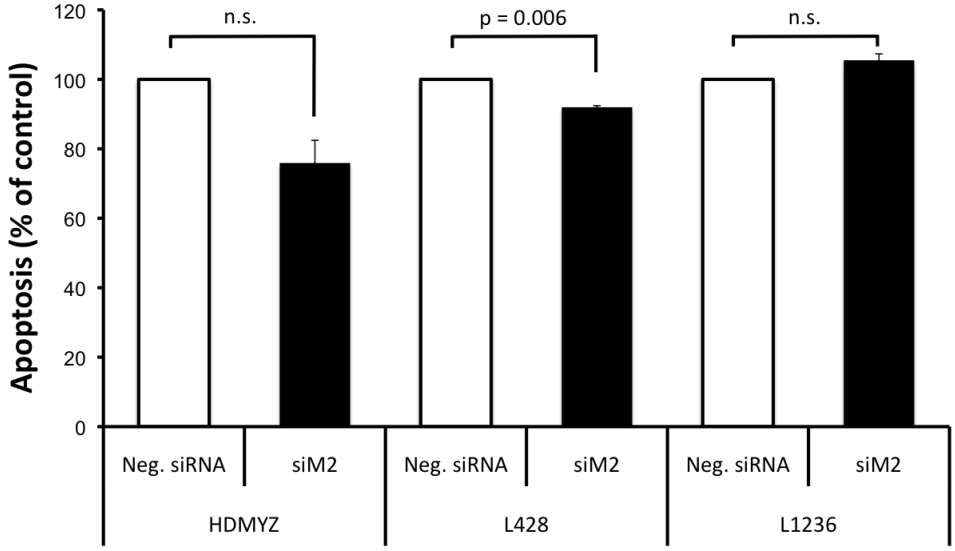

Figure 4.7: Combined results of apoptosis assays of HL cell lines 48h after transient transfection. The combined results of two independent experiments per cell line are shown. Cells were either transfected with neg. siRNA or siM2 and apoptosis was determined after 48h of incubation. Cells were regarded as apoptotic, if they stained positive for only Annexin V-PE or Annexin V-PE and 7-AAD. The error bars indicate standard error of the mean of duplicates.

4.5 Knockdown of MLL5 induces apoptosis after growth factor withdrawal

HRS cells are well known to benefit from cells in the tumor microenvironment, which produce growth factors and thereby promote tumor proliferation and survival (see section 1.1). For this reason we wanted to test, how HL cell lines would react, if these proliferative stimuli were withdrawn in vitro by absence of growth factor containing FBS in the culture medium. Therefore, cells were treated with either neg. siRNA or siM2 and incubated in standard medium for 48h in a humidified atmosphere. Then, cells were removed from the medium and spread in new 6-well plates with serum-free medium for another 72h of incubation. Finally, apoptosis was examined using the Annexin V-PE Apoptosis Detection Kit I (see section 3.9).

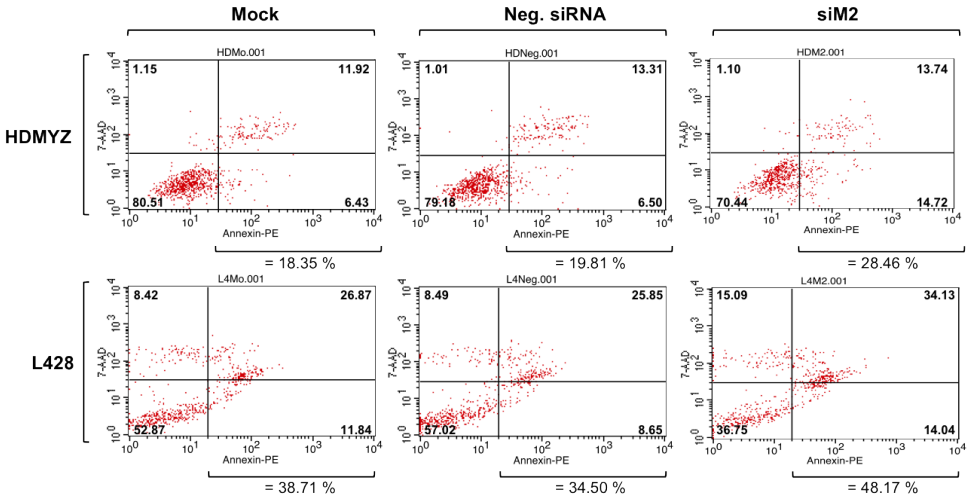

Figure 4.8: FACS analyses of apoptosis assays of MLL5 siRNA treated HDMYZ and L428 cells and control cells after serum starvation. Density dot plots that display 10% of total cell counts (20.000 events) of mock (no siRNA), neg. siRNA, and siM2 transfected HDMYZ (upper panel) and L428 (lower panel) cells are shown. Viable cells are presented in the left lower quadrant, whereas apoptotic cells are shown in the right upper and lower quadrant of each diagram. The numbers in the quadrants are percentages of total gated events. The numbers below the diagrams mark the percentage of apoptotic cells.

Figure 4.8 shows flow cytometry data of one apoptosis assay of HDMYZ and L428, respectively. As can be seen, there was only a slight difference in apoptosis between mock and neg. siRNA transfected cells, but there were higher apoptosis rates in MLL5 knockdown cells of both cell lines tested. In HDMYZ apoptosis was about 44% higher

in siM2 treated cells, than in cells treated with neg. siRNA, and in L428 apoptotic rates were about 40% higher in MLL5 knockdown cells. The consistently higher rates of apoptosis in L428 can be explained by electroporation as method to deliver siRNAs, which is usually more likely to damage cells than transfection by lipofection.

In order to validate the observed changes in cell viability, experiments were replicated two more times in the same way. Combined results of these three independent experiments are displayed in figure 4.9. As shown, there was a statistically higher apoptosis of 30% in siM2 treated HDMYZ cells than in neg. siRNA treated cells. The higher apoptosis rates in L428 could only be reproduced partially. Thus, there was a higher apoptosis of about 15% in L428 MLL5 knockdown cells as compared to controls, but due to variations in the experiments this difference was not statistically significant. However, this result is interesting, considering the results of previous experiments that showed a lower apoptosis in L428 MLL5 knockdown cells 48h after transfection without further treatment (see section 4.4).

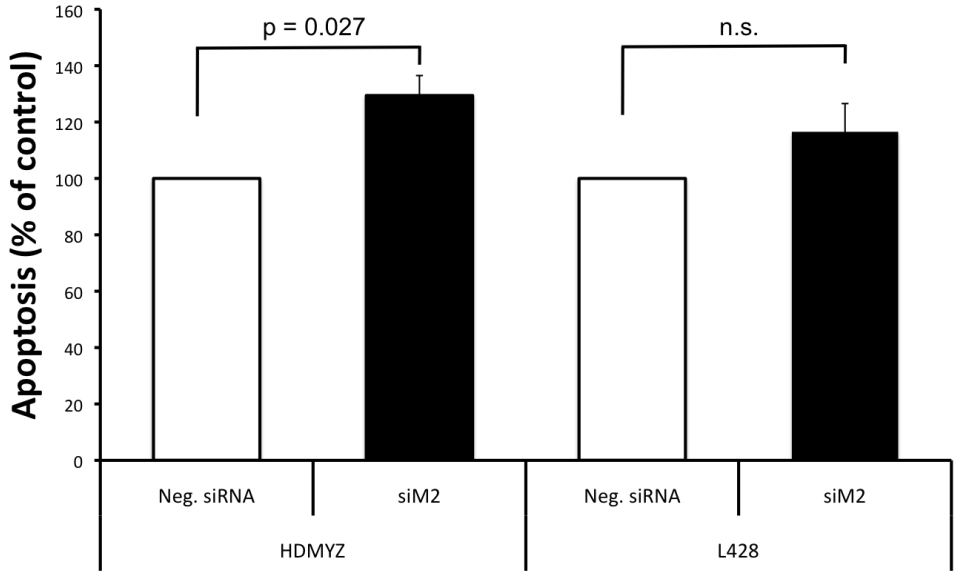

Figure 4.9: Combined results of apoptosis assays of HDMYZ and L428 after serum starvation for 72h. The combined results of three independent experiments per cell line are shown. Cells were transfected with either neg. siRNA or siM2, incubated for 48h, and finally apoptosis was determined after 72h of serum starvation. Cells were regarded as apoptotic, if they stained positive for only Annexin V-PE or Annexin V-PE and 7-AAD. The error bars indicate standard error of the mean of triplicates.

4.6 MLL5 down-regulation enhances responsiveness of L1236 to chemotherapy agent etoposide

To test whether MLL5 influences chemoresistance of HL cells, apoptosis was determined after treatment with chemotherapy agent etoposide using the Annexin V-PE Apoptosis Detection Kit I. For this analyses we referred to Steage et al. (2008), who analyzed gene expression profiles of HL cell lines with a different responsiveness to chemotherapy. Therefore cell line L1236 was chosen for further analyses, as it showed the lowest sensitivity for all tested drugs in their study. Cells were transiently transfected with MLL5 targeting siRNA or neg. siRNA and incubated for 48h. Then, 10 μg/ml of topoisomerase II inhibitor etoposide, diluted in DMSO, was added to the cells. Apoptosis was determined by flow cytometry after another 24h of incubation. Figure 4.10 shows the combined data of two independent experiments. As can be seen, there was a statistically significant reduction in cell viability of about 15% in MLL5 knockdown cells as compared to cells treated with neg. siRNA.

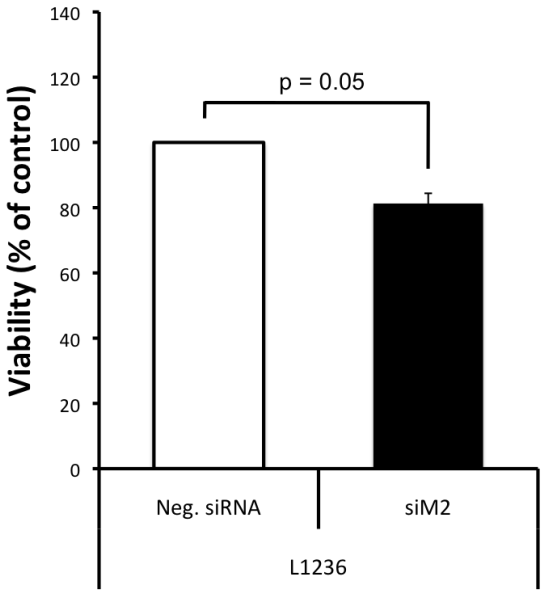

Figure 4.10: Combined results of chemotherapy-induced cell death of L1236 after etoposide treatment for 24h. The combined results of two independent experiments are shown. L1236 cells were transfected with either neg. siRNA or siM2, incubated for 48h, and finally cell viability rates were determined 24h after addition of etoposide. Cells were regarded as viable, if they stained negative for both Annexin V-PE and 7-AAD. The error bars indicate standard error of the mean of duplicates.

This result may implicate an enhanced sensitivity of MLL5-suppressed L1236 cells towards etoposide-induced cell death. Nevertheless, further studies with additional cell lines and modified concentrations have to follow in order to draw the right conclusions.

4.7 MLL5 knockdown alters morphology of HDMYZ cells

After siRNA mediated knockdown of MLL5 in semi-adherent HDMYZ cells, morphological disparities in size and shape of cells could be observed. As shown in figure 4.11, neg. siRNA treated HDMYZ cells displayed a large dendritic shape, which is typical for many adherent cell lines. MLL5 knockdown cells, on the contrary, usually showed a morphological rounding of cells without formation of cellular protrusions, but still grew adherent.

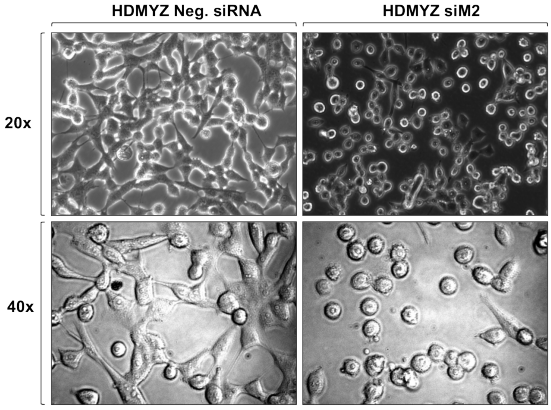

Figure 4.11: Light microscopical images of morphological alterations in HDMYZ after MLL5 knockdown. HDMYZ cells were treated with either neg. siRNA (left column) or siM2 (right column) and incubated for 48h, before morphology was evaluated at low magnification (20x and 40x) under a Zeiss AxioVert 100 light microscope.

The same experiment was replicated one more time with equal results. However, the nature of these morphological changes and possible reasons, such as cytoskeletal changes or multinucleation, as a cause for changes in cell shape and size, need further evaluation. Unfortunately, cell cycle analyses performed with HDMYZ knockdown and control cells were inconclusive and are therefore not shown here.

4.8 Effect of MLL5 knockdown on cellular gene expression profile of L1236

4.8.1 Top differentially regulated genes after MLL5 knockdown

To identify possible downstream targets of MLL5, microarray analyses of MLL5 knockdown cells and control cells, transfected with neg. siRNA, were performed. Therefore, RNA of transiently transfected L1236 cells, treated with either siM2 or neg. siRNA, was isolated 60h after transfection and subjected to microarray analyses on Affymetrix GeneChip®Human Gene 1.0 ST Arrays (see section 3.11).

Figure 4.12 shows heatmaps of microarray data from neg. siRNA treated L1236 (K1, K2) and siM2 treated cells (siM2_1, siM2_2). The left panel displays the 60 most up-regulated genes after knockdown of MLL5, whereas the right panel shows the 60 most down-regulated genes. As highlighted with the black arrow, microarray data confirmed reduction of MLL5 expression after treatment of cells with siM2, as demonstrated before by qRT-PCR. Moreover, the white arrow flags GAPDH and ACTB, two housekeeping genes, which were used as standards for normalization in qRT-PCR (GAPDH) or Western blot analyses (ACTB). Both genes didn't show regulation upon treatment with siM2 and therefore proved to be valid as standards. Interestingly, among the most down-regulated genes there were several genes, which are known to be involved in tumor invasion and metastasis, such as the kinesin family member 18A (KIF18A) or the ribosomal protein S27 (RPS27) (indicated by green arrows) (Nagahara et al. 2011, Wang et al. 2006, Zhang et al. 2010). Another group of coding and non-coding RNAs (ncRNAs), within those down-regulated upon MLL5 knockdown, are involved in post-transcriptional modifications of different RNA types. On the one hand, small nucleolar RNAs (snoRNAs), a group of ncRNAs required for post-transcriptional nucleotide modifications of ribosomal RNAs and small nuclear RNAs (Ono et al. 2011), and on the other hand, RNPC3 (RNA-binding region containing 3) and LSM5 (LSM5 homolog, U6 small nuclear RNA associated) that encode for proteins associated with human spliceosome complexes, which facilitates pre-mRNA splicing (Benecke et al. 2005, Salgado-Garrido et al. 1999).

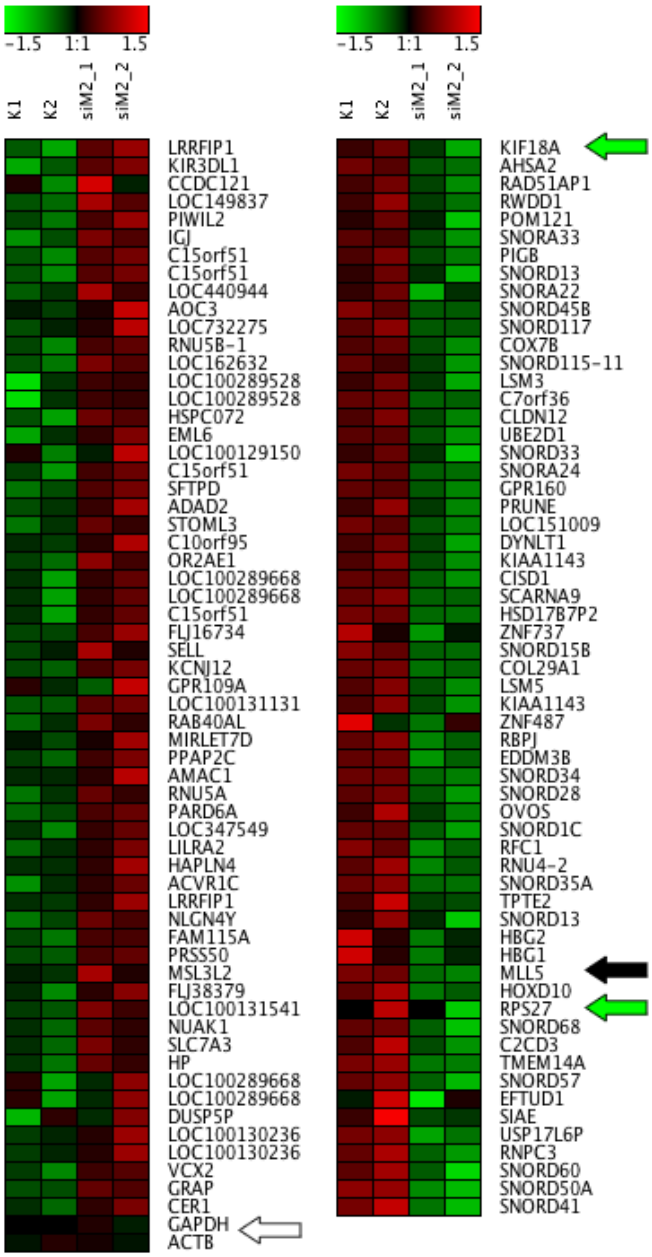

Figure 4.12: Microarray data of MLL5 siRNA treated L1236 cells and control cells 60h after transfection. Heatmaps show $\log_2$ transformed median-centered signal intensities of two technical replicates of one experiment. Each column represents one individual array. Red color indicates higher expression, black color unchanged expression, and green color lower expression between control samples (K1, K2) and MLL5 knockdown samples (siM2_1, siM2_2), as illustrated in the bars above the heatmaps. **Left panel:** Top 60 up-regulated genes in MLL5 knockdown cells compared to controls are shown. The white arrow highlights GAPDH and ACTB, two housekeeping genes with an unchanged expression after knockdown. **Right panel:** Top 60 down-regulated genes in MLL5 knockdown cells compared to controls are shown. The black arrow highlights MLL5, whereas the green arrows flag genes involved in tumor invasion and metastasis.

In order to evaluate the importance of down-regulated genes after MLL5 knockdown, interesting candidates, such as the genes involved in invasion and metastasis (KIF18A and RPS27), were reviewed for differential expression in HL cell lines and benign tissues using microarray analyses. These microarray analyses of HL cell lines and several benign B cell samples were already performed for other investigations by Günther Richter and other members of the Children's Cancer Research Center (Technical University of Munich) using Affymetrix GeneChip®Human Genome U133A arrays, containing 22,000 oligonucleotide probe sets for about 14,500 genes.

One of the above mentioned genes, the kinesin family member 18A (KIF18A), was identified to be expressed at higher levels in all HL cell lines (red bars), as compared to normal B cells and several other normal tissues (black bars) (see figure 4.13).

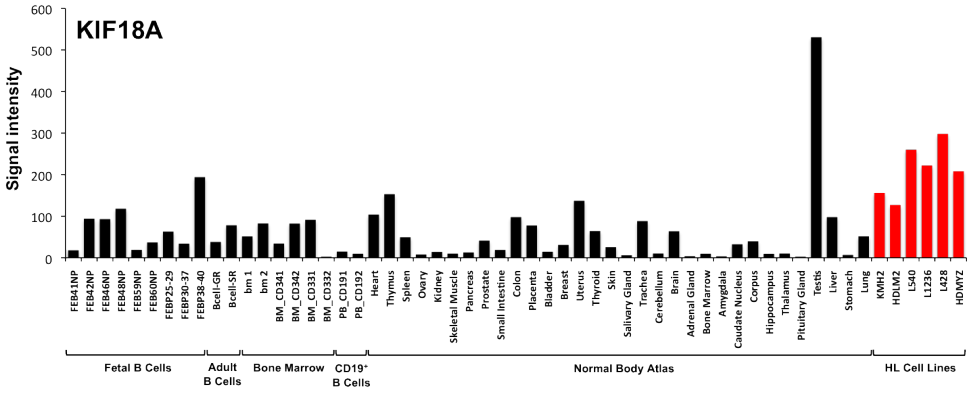

Figure 4.13: Microarray data of mRNA expression of KIF18A in HL cell lines and benign tissues. Expression of KIF18A on mRNA level was analyzed by microarray analyses on GeneChip®Human Genome U133A arrays for HL cell lines (red bars), hematopoietic tissues (fetal B cells, adult B cells, bone marrow cells and $CD19^+$ B cells) and several other normal tissues (normal body atlas) (black bars). Microarray data from one KIF18A reporter is shown.

In order to verify the down-regulation of KIF18A upon MLL5 knockdown, as observed in microarray analyses of L1236, qRT-PCR analyses of MLL5 knockdown cells, using a specific KIF18A gene expression assay, were performed. As KIF18A mRNA levels were also high in other HL cell lines, L428 and HDMYZ were chosen for independent verification. As shown in figure 4.14, KIF18A was down-regulated about 25–40% in both L428 and HDMYZ upon knockdown of MLL5, as already indicated by microarray analyses of L1236 MLL5 knockdown cells.

In summary, KIF18A seems to be overexpressed in several HL cell lines as compared

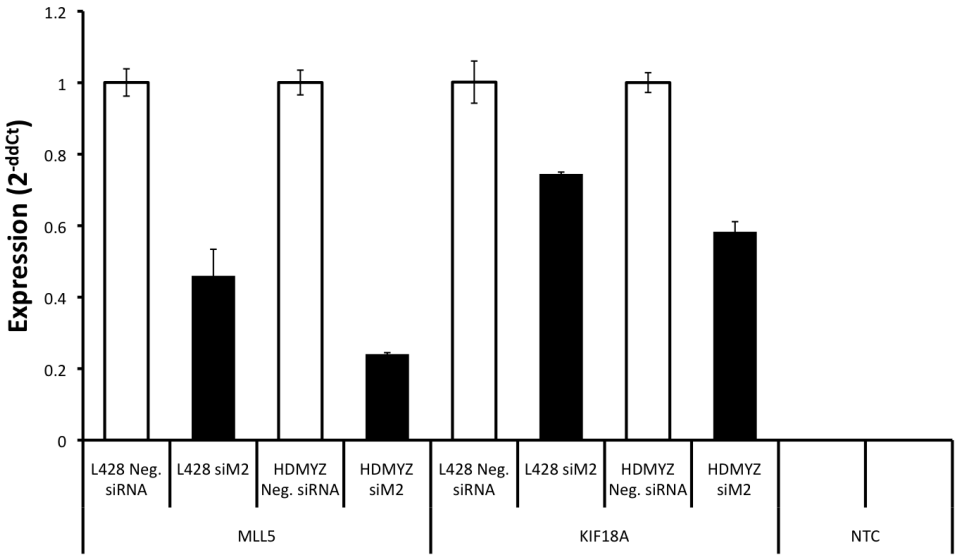

Figure 4.14: Quantification of MLL5 and KIF18A mRNA levels upon knockdown of MLL5 in L428 and HDMYZ by qRT-PCR. MLL5 and KIF18A mRNA expression is shown in two HL cell lines (L428 and HDMYZ) treated with either specific MLL5 targeting siRNA (siM2) or neg. siRNA. Analyses were performed 60h after transient transfection. NTC, non-template control (H_2O).

to normal tissues, and its expression seems to be directly or indirectly regulated by MLL5. However, the disease contribution of KIF18A, which is already implicated in invasion and metastatic spread, needs further in vitro and in vivo evaluation, e.g. by invasion assays after knockdown of MLL5 and KIF18A, respectively.

4.8.2 Effect of MLL5 knockdown on lineage promiscuity gene expression

It is well known that HRS cells aberrantly express several markers of other hematopoietic lineages (see section 1.1). Keeping in mind that MLL5 is implicated in the development of several hematopoietic lineages (see section 1.2), we wanted to investigate the effects of MLL5 knockdown on the expression of lineage-inappropriate genes in HL cell lines. For this reason, we scanned through the microarray analyses of L1236 and found several genes, which are aberrantly overexpressed in HRS cells, among the down-regulated genes after MLL5 knockdown. The following table shows a selection of

genes with a lower expression in siM2 treated L1236 cells as compared to neg. siRNA treated cells.

Table 4.1: Genes from microarray analyses of siM2 treated L1236 cells, which are known to be overexpressed in HL, and down-regulated after MLL5 knockdown. Genes with a known overexpression in Hodgkin lymphoma, their function and the reference are shown. Negative linear fold changes stand for lower expression in siM2 treated L1236 cells as compared to neg. siRNA treated cells. Data is mean and standard error of the mean of the ratios of gene expression in siM2 treated cells to expression in neg. siRNA treated cells of two technical replicates per sample. Reduced expression of MLL5 is indicated as reference value.

Gene	Linear FC	Function	Reference
MLL5	-0.47 ± 0.01		
IL6	-0.31 ± 0.02	Inflammatory cytokine	Reynolds et al. (2002)
ID2	-0.24 ± 0.06	Inhibition of differentiation	Mathas et al. (2006)
ATF5	-0.21 ± 0.04	Transcription factor	Schwering et al. (2003)
CD58	-0.20 ± 0.12	Activation of T cells	Schmitz et al. (2009)
IL5RA	-0.19 ± 0.05	Cytokine receptor	Staege et al. (2008)
IL1R2	-0.19 ± 0.01	Cytokine receptor	Ma et al. (2008)
GATA3	-0.17 ± 0.12	T cell development	Stanelle et al. (2010)
BIRC3	-0.17 ± 0.05	Inhibitor of apoptosis	Dürkop et al. (2006)
CD40	-0.16 ± 0.06	Activation of NF-κB	Küppers (2009)
BMI1	-0.12 ± 0.04	Cell development	Raaphorst et al. (2000)
EZH2	-0.10 ± 0.07	Cell development	Raaphorst et al. (2000)

As can be seen in table 4.1, among the genes down-regulated upon MLL5 knockdown, there were several genes, which have already been described in the introduction as pivotal for HL pathogenesis, such as GATA3, ID2, CD40, or the HSC genes BMI1 and EZH2 (see section 1.1).

In order to validate the observed changes in gene expression by qRT-PCR analyses, primer assays for GATA3, EZH2 and BMI1 were obtained. Surprisingly, gene expression data could not be verified in L1236. However, a reduction of 30–35% in mRNA levels of EZH2, BMI1, and GATA3 could be detected in HDMYZ after MLL5 knockdown, as shown in figure 4.15.

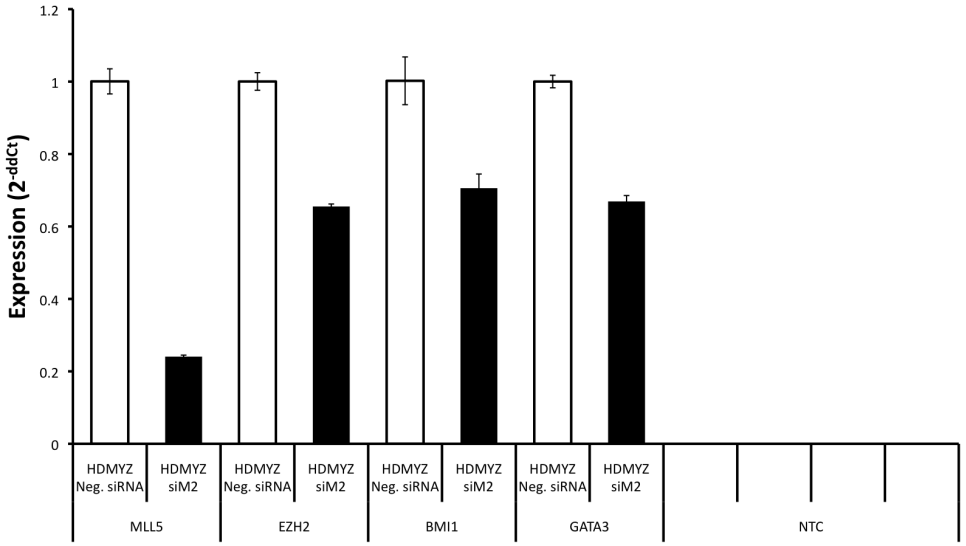

Figure 4.15: Quantification of MLL5, EZH2, BMI1, and GATA3 mRNA levels upon knockdown of MLL5 in HDMYZ by qRT-PCR. MLL5, EZH2, BMI1, and GATA3 mRNA expression is shown in HDMYZ cells treated with either specific MLL5 targeting siRNA (siM2) or neg. siRNA. Analyses were performed 60h after transient transfection. NTC, non-template control (H_2O).

4.8.3 Effect of MLL5 knockdown on expression of genes with a possible contribution to chemoresistance of L1236

As already mentioned above, MLL5 knockdown enhanced sensitivity of L1236 cells towards etoposide-induced cell death (see section 4.6). For this reason, we analyzed the microarray data and looked for possible changes in gene expression after MLL5 knockdown that might contribute to explaining this phenotype. We found an interesting correlation between down-regulated genes after MLL5 knockdown and genes that showed a higher expression in chemoresistant L1236 as compared to chemosensitive L540 (for microarray analyses of differentially expressed genes between L1236 cells and L540 cells see Staege et al. (2008) figure 4). Among those 11,336 genes (out of

a total of 28,869 genes on the Affymetrix GeneChip®Human Gene 1.0 ST Arrays) down-regulated in L1236 after MLL5 knockdown, 29 out of the 43 genes that might be related to chemoresistance of L1236 were present (genes mentioned twice in the reference paper were not considered). The reduced expression of MLL5 and the other genes is shown in figure 4.16.

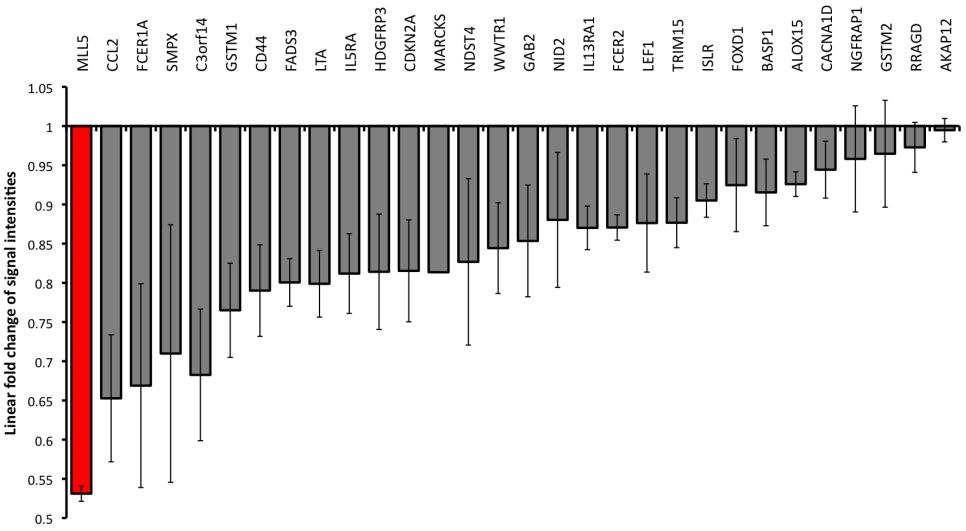

Figure 4.16: Overview of genes that might be associated with chemoresistance of L1236 and their expression after MLL5 knockdown. The expression of 29 out of 43 genes that might be associated with chemoresistance of L1236, as mentioned in the analyses of Staege et al. (2008), is shown after knockdown of MLL5. The red bar indicates reduced expression of MLL5 as a reference value. The linear fold changes of signal intensities are mean of the ratios of gene expression in siM2 treated cells to expression in neg. siRNA treated cells of two technical replicates per sample. Error bars are standard error of the mean.

Several interesting genes could be identified among those down-regulated upon MLL5 knockdown, such as the glutathione S-transferase mu 1 (GSTM1), which functions in the detoxfication of certain therapeutic drugs, e.g. alkylating agents or platinum compounds, and therefore might affect their efficiency, CD44 a cell-surface glycoprotein that is involved in lymphocyte activation and tumor metastasis, or the myristoylated alanine-rich protein kinase C substrate (MARCKS), which seems to contribute to cisplatin-resistance of ovarian carcinoma cells (Righetti et al. 2006).

The venn diagram in figure 4.17 illustrates the significance of overlap between the genes down-regulated upon MLL5 knockdown and those, which might facilitate chemoresistance of L1236 cells (for statistical analysis see section 3.12).

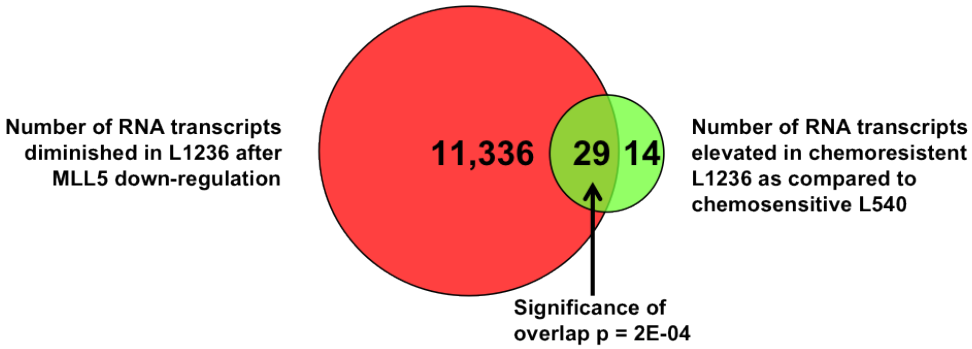

Figure 4.17: Venn diagram showing an overlap between genes down-regulated after MLL5 knockdown and those that might be associated with chemoresistance of L1236. In each circle is reported the number of genes present in the list. For the intersection is reported the size and significance of overlap (Fisher's Exact Test).

However, if the observed phenotype was really due to these changes in gene expression or if other factors were accountable for the increased sensitivity towards etoposide needs further evaluation.

4.9 Knockdown of MLL5 modifies histone 3 (H3) methylation and acetylation status

Since MLL5 and other members of the mixed lineage leukemia family were reported to directly or indirectly mediate methylation of histone 3 at lysine 4 (H3K4), global levels of these activating histone modifications were assessed after knockdown of MLL5 by Western blot analyses. Besides di- and trimethylation of histone 3 at lysine 4 (H3K4me2/me3), acetylation of histone 3 was evaluated, since TrxG multiprotein complexes may recruit HATs, which acetylate histone tails and thereby support activation of gene expression (see section 1.2). In order to analyze changes in histone methylation and acetylation, cells were transiently transfected with either siM2 or neg. siRNA and incubated for 60h at 37°C with 5% CO_2 in a humidified atmosphere. Then, whole protein lysates were prepared, and Western blot analyses were performed, as described in section 3.7. For validation of MLL5 knockdown efficiency, RNA of knockdown and control samples was isolated and qRT-PCR analyses were performed.

As can be seen in figure 4.18, transient knockdown of MLL5 resulted in a global decrease of H3K4me3 and to a minor degree H3K4me2 in all three cell lines tested. Moreover, transient down-regulation of MLL5 also decreased acetylation of histone 3 at lysine 9 and lysine 14 (H3K9/K14Ac) in HDMYZ and L428.

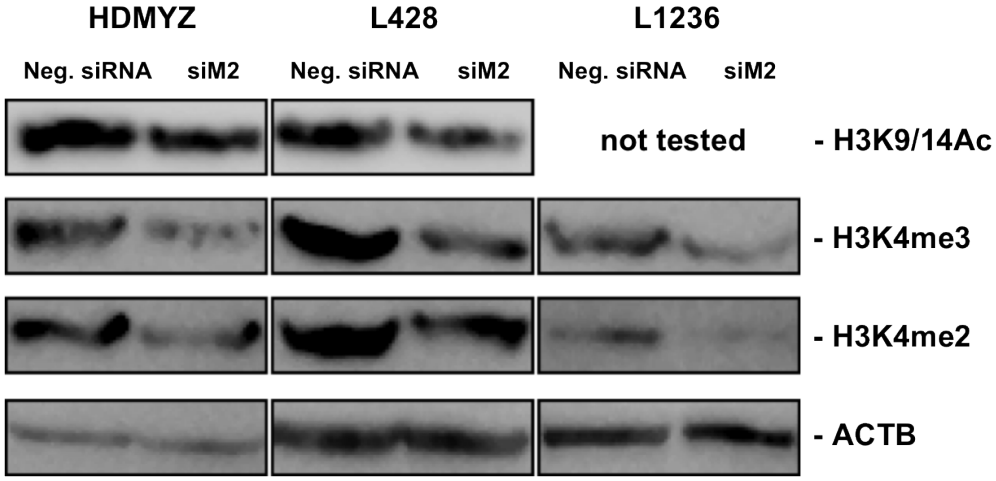

Figure 4.18: Evaluation of global histone methylation and acetylation status 60h after transient down-regulation of MLL5 in different HL cell lines by Western blot analyses. Specific antibodies against H3K4me2, H3K4me3, and H3K9/14Ac were used to evaluate changes in histone modifications between cells treated with either neg. siRNA or siM2. Detection of ACTB protein amounts served as loading control.

These results indicated that there was a global reduction in activating chromatin modifications upon knockdown of MLL5. However, the underlying mechanisms, e.g. through a direct methyltransferase activity of MLL5 or through indirect utilization of further chromatin modifiers, remains ambiguous.

5 Discussion

5.1 Disease contribution of TrxG protein MLL5 in classical Hodgkin lymphoma

The classical HL is characterized by sporadic tumor cells, the Hodgkin and Reed-Sternberg cells, within an inflammatory microenvironment. Despite their B cell origin these tumor cells display a dramatic deregulation in lineage affiliation, with restricted expression of B cell markers and aberrant expression of multiple markers of other hematopoietic cells. In order to gain further insights in the deregulated transcriptome of these tumor cells, we used a new approach, which allowed us to compare total mRNA expression of primary HRS cells and healthy control cells. As opposed to conventional analyses, where about 1,000 or more HRS cells were necessary for amplification and subsequent microarray analysis (Karube et al. 2006), we needed as little as 1–30 tumor cells. Our analyses verified several genes, which were already implicated in HL oncogenesis or which are part of cellular pathways with a known disease contribution, such as the NF-κB or JAK-STAT pathway (Mollweide et al. manuscript in preparation). However, given that a lot of studies already focused on these established features of HL, we intended to illuminate new putative key players and therefore looked for genes, which might contribute to some of the most striking features of HRS cells, such as the expression of lineage-inappropriate genes or the multinucleation of tumor cells.

The TrxG family member MLL5, which was among those genes with a higher expression in HL as compared to germinal center B cells in our analyses (see figure 4.1), was picked as a promising target of research, as recent studies proved its critical role in stem cell regulation and differentiation of hematopoietic precursors (Liu et al. 2009). Deregulation of TrxG family members have already been implicated in a number of

hematopoietic malignancies, especially myeloid and lymphoid leukemias (Mills 2010). Yet, as opposed to PcG proteins, such as EZH2 and BMI1, which might play an important role in epigenetic down-regulation of B cell factors in HRS cells, TrxG proteins have not been mentioned in HL pathogenesis, so far. This study shows for the first time that a MLL family member is deregulated in HL, and that knockdown of MLL5 led to severe phenotypical changes in HL cell lines.

5.1.1 Knockdown of MLL5 influences both proliferation and apoptosis of HL cells

In order to characterize changes in the behavior of HL cell lines upon MLL5 knockdown, proliferation and apoptosis assays were performed. BrdU incorporation assays showed a significantly decreased proliferation of HL cell lines after siRNA mediated RNAi against MLL5 (see figure 4.6). These changes were most likely due to cell cycle alterations, as no increased spontaneous apoptosis was measured after MLL5 down-regulation (see figure 4.7). Similar results were obtained by Cheng et al. (2008), who showed a decreased proliferation of human cervical carcinoma (HeLa) and osteosarcoma (U2OS) cells after knockdown of MLL5. They explained these observations by induction of cell cycle arrest at both G_1/S and G_2/M phase upon RNAi. In addition, MLL5 down-regulation led to p53-independent up-regulation of cell cycle inhibitor p21 and dephosphorylation of the retinoblastom protein, which might to some extent contribute to cell cycle arrest (Cheng et al. 2008).

More recent studies from the same laboratory further characterized the role of MLL5 in cell cycle regulation. They found that the central domain of MLL5 is phosphorylated during mitosis by the CDK1/cyclin B1 (cyclin-dependent kinase 1/cyclin B1) complex, and that this modification is required for mitotic entry (Liu et al. 2010). Interestingly, both CDK1 and cyclin B1 are also overexpressed in Hodgkin lymphoma (Bai et al. 2005). This leads to the hypothesis, that MLL5 might, as a substrate of the CDK1/cyclin B1 complex, contribute to the cell cycle regulation in HRS cells and therefore facilitate cell cycle progression, especially at the G_2/M check point. Vice versa knockdown of MLL5 or inhibition of phorphorylation might lead to cell cycle partial arrest at this control point.

Another crucial cell cycle regulator is the tumor suppressor protein p53. Multiple analyses showed a high expression of unmutated p53 in primary HRS cells, yet p53 was somehow unable to induce cell cycle arrest (Montesinos-Rongen et al. 1999, Pasman et al. 1994). Overexpression of MLL5 in HRS cells might, at least partially, explain this controversy, as Cheng et al. (2011) showed that chromatin-bound MLL5 prevented binding of p53 to loci of downstream genes, and that degradation of MLL5 enabled p53 binding and target gene transcription (Cheng et al. 2011). However, it was also shown that, as opposed to HDMYZ, L1236 and L428 harbor truncated and transcriptionally inactive p53 proteins, excluding the latter explanation as a likely reason for decreased proliferation of these cells (Feuerborn et al. 2006, Janz et al. 2007). In summary, it is conceivable that MLL5 might apply p53-dependent and p53-independent mechanisms to restrain cell cycle progression. Yet, further in vitro analyses need to be performed, to provide deeper insights in the mechanisms behind the inhibition of proliferation of HL cells upon MLL5 knockdown.

In this study, no increased spontaneous apoptosis could be detected after knockdown of MLL5 in three HL cell lines (see figure 4.7). Since primary HRS cells are dependent on anti-apoptotic and proliferative stimuli from the tumor microenvironment, through both receptor-ligand interaction and secretion of cytokines and growth factors, we concluded that HL cells in vitro might also benefit from external factors in the culture medium. Therefore, we intended to trigger apoptosis by growth factor deprivation through serum withdrawal (Ashida et al. 2011, Lu et al. 2008). Tumor cells often apply several internal signal cascades upon growth factor withdrawal in order to escape apoptosis. If these internal signals are blocked, e.g. after RNAi, tumor cells can no longer provide these survival signals and apoptosis can be induced (Ming et al. 2008). For this reason, serum starvation is a powerful tool to reveal changes in the balance between pro- and anti-apoptotic factors, which might be hidden by excessive external growth factor stimulation. Our experiments showed a significantly higher apoptosis rate in serum-starved HDMYZ cells, yet the higher apoptosis rates in L428 were not statistically significant (see figure 4.9). This suggested that MLL5 knockdown could have altered intrinsic survival pathways in the tumor cells, and that withdrawal of proliferative stimuli might therefore have caused an increased apoptosis rate. It is also supposable that activation of p53 could initiate apoptosis in HDMYZ, which, as opposed to L428, shows specific p53 transcripts (Bargou et al. 1993).

Besides initiation of apoptosis triggered by serum starvation, a higher sensitivity towards chemotherapy agent etoposide could be detected in the HL cell line L1236. MLL5 knockdown cells showed a statistically significant reduction in cell viability as compared to control cells (see figure 4.10). Interestingly, L1236 was described as one of the most chemoresistant HL cell lines by Steage et al. (2008), who treated several HL cell lines with cisplatin, etoposide, and melphalan and investigated cell viability. In order to explain this phenotype, the group tried to identify genes associated with resistance against chemotherapy agents in HL cell lines. Therefore, they performed gene expression analyses of chemoresistant L1236 and chemosensitive L540. These analyses identified a number of differentially expressed genes, some of which are already described in the context of drug metabolism or chemoresistance, such as GSTM1 or MARCKS (Staege et al. 2008). Comparing our microarray analyses of L1236 MLL5 knockdown cells to their analyses, we found a significant overlap between genes, which are down-regulated upon MLL5 knockdown and genes with a possible contribution to chemoresistance of L1236 cells (see figures 4.16 and 4.17). This might implicate that MLL5 directly or indirectly up-regulates several factors that support chemoresistance, and that these factors at least partially vanish after MLL5 down-regulation and therefore endorse initiation of apoptosis. Nevertheless, further analyses have to be provided in order to consolidate these findings, and highlight the role of MLL5 in anti-apoptosis in HL cell lines.

5.1.2 MLL5 down-regulation alters cellular gene expression profile of HL cells

To reveal putative downstream target genes of mixed lineage leukemia 5, microarray analyses of MLL5 knockdown cells and control cells were performed for HL cell line L1236. Among the top differentially expressed genes there were several, which might link MLL5 to tumor invasiveness and migratory potential, such as RPS27 or KIF18A (see figure 4.12). The kinesin family member 18A, which was down-regulated upon MLL5 knockdown, is a microtubule-associated motor protein that contributes to microtubule depolymerization and microtubule-based movement, two pivotal requirements for cell migration (Mayr et al. 2007, Zhu et al. 2005). Two recent studies reported an overexpression of KIF18A in breast cancer and colorectal cancer (Nagahara et al.

2011, Zhang et al. 2010). Nagahara et al. (2011) showed that a higher expression of KIF18A in colorectal tumor tissues as compared to normal tissues was significantly correlated with primary tumor stage, lymph node metastasis, lymphatic, and venous invasion. Moreover, in vitro analyses confirmed a reduced proliferation, cell migration, and invasion upon KIF18A knockdown (Nagahara et al. 2011). Zhang et al. (2010) observed similar results in human breast cancer, where KIF18A overexpression was significantly correlated with advanced tumor grade, existence of distant metastasis, and poor overall survival. As KIF18A was also implicated in mitotic processes, such as formation of the spindle apparatus with subsequent chromosome segregation and cell migration during interphase (Mayr et al. 2007, Stumpff et al. 2008), the group performed in vitro assays to assess the effects of up- and down-regulation of KIF18A on cell division. They found that ectopic overexpression of KIF18A in breast cancer cells resulted in multinucleation, which is, by the way, also one of the most characteristic features of HL tumor cells. In contrast, KIF18A knockdown led to reduced proliferation, most likely due to G_2/M phase arrest caused by perturbations of mitotic spindle function and interphase dynamics (Zhang et al. 2010).

In order to investigate a possible disease contribution of KIF18A in HL we scanned through existing microarray analyses of HL cell lines and benign tissues, and found that KIF18A expression was higher in all HL cell lines as compared to benign hematopoietic tissues and other normal tissues (see figure 4.13). Down-regulation of KIF18A upon RNAi against MLL5, as seen in microarray analyses of L1236, was then validated for two more HL cell lines, L428 and HDMYZ (see figure 4.14). So far, we concluded that high MLL5 expression in HL cell lines might enhance KIF18A expression and therefore might contribute to invasive potential of tumor cells. Interestingly, two reports already linked MLL5 to metastatic behavior in prostate cancer and human melanoma (Chandran et al. 2007, Winklmeier et al. 2009). Chandran et al. (2007) analyzed gene expression profiles of primary prostate tumor samples and metastatic samples, and found that MLL5 was among the top 100 genes up-regulated in the metastasis. Furthermore, Winklmeier et al. (2009) showed that MLL5 expression increased during melanoma progression from melanoma-in-situ, via the radial growth phase of the tumor, to lymph node metastasis.

Cytoskeletal changes, due to perturbations in the microtubule dynamics after KIF18A

down-regulation upon MLL5 knockdown in HDMYZ, might also account for the morphological changes observed in this cell line after RNAi (see figure 4.11).

According to this data, we suggested that MLL5 overexpression might contribute to metastatic progression of HL cells, at least in part by up-regulation of KIF18A or other factors. An increase in MLL5 expression during tumor progression, as seen in human melanomas, might also explain the broad variation of MLL5 mRNA levels in the primary HL tumor samples used for the microarray analyses in this study (see figure 4.2). Thus, some of the lymph node biopsy specimens might be part of the initial tumor with lower MLL5 expression, whereas other samples might have derived from lymph node metastasis, which might express higher levels of MLL5. However, as opposed to solid tumors, differentiation between primary tumor location and metastasis is tricky in lymphomas. Nevertheless, we are aware of the fact that much more in vitro data, e.g. by invasion assays after MLL5 and KIF18A knockdown, is necessary in order to corroborate the hypotheses established from the microarray data.

Based on the role of MLL5 in hematopoietic development and lineage differentiation we also looked for changes in the expression of genes, which are aberrantly overexpressed in HL cells, but usually show a low expression in normal B cells. Among the down-regulated genes after MLL5 knockdown we found several genes with an established role in the pathogenesis of Hodgkin lymphoma (see table 4.1). One of them is interleukin 6, a cytokine with a high expression in HRS cells, which contributes to the formation of the inflammatory microenvironment, and of which elevated levels are associated with a bad treatment outcome (Nagel et al. 2005, Reynolds et al. 2002). Another one is the transcriptional regulator ID2, which was shown to inhibit the function of TCF3 (E2A), a critical B cell-determining transcription factor and thus prevents the transcription of B cell specific genes, which again contributes to the characteristic loss of the B cell phenotype (Mathas et al. 2006).

5.1.3 Microarray and Western blot analyses provide an insight into possible epigenetic mechanisms of MLL5 in HL cells

As more and more evidence is provided that epigenetic processes might play a major role in HL pathogenesis, we also focused on differential expression of PcG proteins EZH2 and BMI1 after MLL5 knockdown. Both genes are overexpressed in HL and encode for PcG proteins, which facilitate restrictive histone modifications, especially H3K27 trimethylation (Mills 2010, Raaphorst et al. 2000). Recent analyses showed that several promoters of B cell genes, such as CD19, CD79A, or PU.1, are trimethylated at H3K27, which leads to epigenetic silencing of these genes (Seitz et al. 2011). Even though changes in gene expression were only marginal in L1236 microarray analyses, we ordered specific primer assays and evaluated expression of EZH2 and BMI1 in other HL cell lines by qRT-PCR. We confirmed that expression of BMI1 and EZH2 did not change upon knockdown of MLL5 in L1236, but we found a reduced expression of both genes upon RNAi against MLL5 in HDMYZ (see figure 4.15). These analyses may indicate a crosstalk between TrxG and PcG genes in HL cells, even though there may be a more complex interaction within the different cell lines. However, the consequences of the down-regulation of EZH2 and BMI1, especially on the H3K27 methylation status and a possible re-expression of B cell genes in HDMYZ, need further evaluation.

As some reports already implicated the TrxG family member MLL5 in methylation of H3K4 to establish active chromatin marks, we looked for quantitative changes in global histone methylation patterns upon knockdown of MLL5 (Fujiki et al. 2009, Sebastian et al. 2009). We observed a decrease of global levels of activating H3K4 di- and trimethylation upon knockdown of MLL5 in all reviewed HL cell lines (see figure 4.18). Similar results were obtained by Sebastian et al. (2009), who reported an indirect regulation of H3K4me2/me3 in mouse myoblasts by MLL5. Fujiki et al. (2009) showed that a short isoform of MLL5 directly mono- and dimethylated H3K4 in human HL60 promyelocytes. We also detected a global quantitative reduction of acetylation of histone 3 at lysine 9 and lysine 14 (H3K9/14Ac) in HDMYZ and L428 (see figure 4.18). Both histone modifications, H3K4 methylation and acetylation of histone 3, are well known to facilitate transcriptional activation (Mills 2010). In conclusion, it

seems as if MLL5 directly or indirectly facilitates H3K4 di- and trimethylation, and that this subsequently leads to an increased acetylation of lysine residues of histone 3 by HATs, a cross-regulation of histone modifications, which was already described before (Latham and Dent 2007).

Interestingly, a recent study showed that promoters of several genes, such as ID2 or FSCN1, which are atypically up-regulated in HL are acetylated at H3K9/14, whereas those of known B cell genes, such as CD19, CD79A, or PU.1, are deacetylated and H3K27 trimethylated, which prevents their expression (Seitz et al. 2011). In addition to that, another report described a selective up-regulation of B cell inappropriate genes and a down-regulation of B cell genes in normal B cells treated with the HDAC inhibitor trichostatin A (TSA) and the DNA methyltransferase inhibitor 5-aza-deoxycytidine. However, treatment of HL cell lines with TSA and 5-aza-dC did not lead to a re-expression of B cell genes (Ehlers et al. 2008). Considering all these findings, this implies that genes with an aberrant overexpression in HL are acetylated at the promoters in HL cells, but lack promotor DNA methylation. Vice versa, promotors of the aberrantly expressed genes in HL are DNA methylated and not acetylated in B cells.

All of this might suggest, that aberrant MLL5 expression in B cells could lead to an increase in H3K4 di- and trimethylation and H3 acetylation at promotors of lineage-inappropriate genes, which are normally DNA methylated and not acetylated, as mentioned before. Recent reports, describing that an unmethylated H3K4 is necessary for de novo DNA methylation by the Dnmt3a-3L tetramer would coincide with this hypothesis quite well (Cheng and Blumenthal 2008, Hu et al. 2009, Ooi et al. 2007). Moreover, it has been reported that HDAC inhibitor treatment, like the TSA treatment of B cells by Ehlers et al. (2008), may not only increase histone acetylation but also methylation of H3K4 (Huang et al. 2011, Marinova et al. 2011).

To further illustrate this hypothesis, the theoretical contribution of MLL5 in expression of lineage-inappropriate genes in HL cells is shown in figure 5.1. The DNA section in the upper panel represents loci of genes, which are aberrantly up-regulated in HL but DNA methylated and not acetylated in normal B cells and therefore not expressed. The lower panel, in contrast, displays changes at these distinct loci upon treatment with HDAC inhibitor TSA and DNA methyltransferase inhibitor 5-aza-dC (A) as well

as upon aberrant overexpression of mixed lineage leukemia 5 in these B cells (B). After TSA and 5-aza-dC treatment promoters of these HL characteristic genes are acetylated and lack DNA methylation, just as described by Ehlers et al. (2008). Similar modifications might be observed upon MLL5 overexpression in normal B cells. MLL5 could facilitate H3K4 di- and trimethylation and subsequently histone acetylation by recruitment of HATs. Moreover, DNA methylation would be inhibited by methylation of lysine 4 of histone 3.

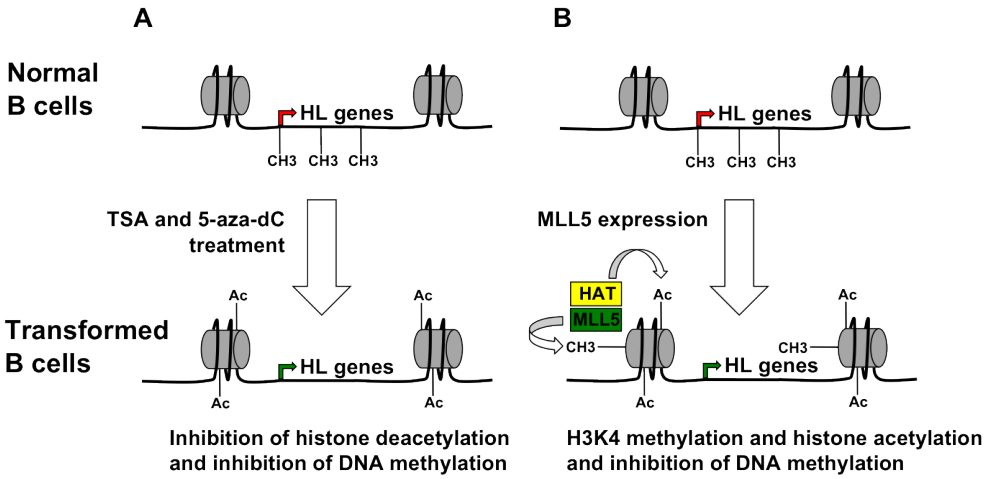

Figure 5.1: Schematic diagram of the potential role of MLL5 in expression of lineage-inappropriate genes in HL cells. A schematic of gene loci of aberrantly expressed genes in HL in normal (upper panel) and transformed B cells (lower panel) are shown. The red arrow indicates no expression of aberrantly expressed genes in HL, whereas the green arrow indicates expression of these genes. **Panel A:** Epigenetic changes at these distinct loci upon treatment of normal B cells with TSA and 5-aza-dC are shown. **Panel B:** Epigenetic changes at these distinct loci upon aberrant overexpression of MLL5 in normal B cells are shown. Ac, histone acetylation; CH3, DNA methylation or H3K4 di- and trimethylation; HL genes, aberrantly expressed genes in HL.

However, the rather remote down-regulation of some aberrantly expressed genes in L1236 upon knockdown of MLL5, as seen in the microarray analyses, supports this hypothesis only partially (see table 4.1). Probably more time, than the 60h of incubation as in the microarray analyses, would be required to see definite changes in gene expression, if one keeps in mind that proliferation of HL cells was severely decreased upon MLL5 knockdown (see figure 4.6). Therefore, it would be crucial to establish constitutive MLL5 knockdown cells with a proper MLL5 down-regulation and monitor gene expression of suspected target genes and histone modifications after an adequate time course. Moreover, further analyses concerning the H3K4 methylation in untreated HL

cells as well as in MLL5 knockdown cells could help to clarify if this activating histone modification is enriched at loci of aberrantly expressed genes.

5.2 Relevance of the data and prospects

The aim of this study was to evaluate the HL disease contribution of MLL5, a TrxG family member, which was identified within a number of genes with a higher expression in primary HL tumor cells than in normal germinal center B cells. The identification and characterization of genes, which are systematically overexpressed in the tumor cells is the foundation for the development of tumor-specific therapy approaches. As long-term toxicities caused by conventional polychemo- and radiotherapy are a huge problem in the treatment of HL, especially in children, this would be of great benefit for the patients.

This work showed for the first time that a MLL family member, namely MLL5, is overexpressed in primary HRS cell, derived from pediatric and adult patients, as compared to their putative cells of origin, the germinal center B cells. Moreover, siRNA mediated RNAi against MLL5 led to a decreased proliferation and an increased apoptosis upon serum withdrawal or treatment with chemotherapy agent etoposide in several established HL cell lines. Microarray analyses revealed that down-regulation of MLL5 affects expression of several genes with a known contribution to tumor invasiveness and metastasis, such as KIF18A, which also seems to be overexpressed in HL cell lines. Furthermore, Western blot and microarray analyses provided an insight into a possible contribution of MLL5 in the epigenetic regulation of the expression of lineage-inappropriate genes in HL. In consideration of all these changes upon MLL5 knockdown, it appears likely that this gene/protein plays a major role in HL oncogenesis.

Even though this work already provided a basis of how HL tumor cells might benefit from MLL5 expression, a lot more work needs to be done to draw the final conclusions. The supposable role of MLL5 in tumor metastasis should be investigated by invasion assays, the enhanced responsiveness towards chemotherapy agents should be further classified, and constitutive MLL5 knockdown cells should be fabricated, in order to clarify, if MLL5 really contributes to the deregulated HL phenoytpe, with aberrant expression of markers of several hematopoietic lineages.

The results shown in this work, especially the assumed epigenetic mechanisms of MLL5 function are interesting, as a lot of novel drugs, such as HDAC inhibitors, 5-aza-dC, or the histone methylation inhibitor DZNep, target epigenetic modifiers (Gore et al. 2006, Miranda et al. 2009, Prince et al. 2009, Zhou et al. 2011). If the hypotheses, which were established in this work, prove true, then MLL5 might become a new interesting candidate for targeted therapy.

In conclusion, the results of this study cleared the way for further specific research concerning the contribution of MLL5 in the pathogenesis of this extraordinary disease. The goals of this work were reached, insofar as a lot of features of the MLL5 knockout phenotype were characterized, and theses results indicate a disease contribution of MLL5 that justifies further distinct analyses.

6 Summary

Hodgkin lymphoma (HL) is a lymphoid malignancy with an annual incidence of about three cases per 100,000 persons and a bimodal disease distribution with peaks at ages 15–34 years and over 60 years. It is characterized by rare specific tumor cells, the Hodgkin and Reed-Sternberg (HRS) cells, which acount for only 1% of cells in affected lymph nodes (LNs), whereas the bulk of the tumor consists of benign immune cells, which form an inflammatory microenvironment. Even though the HRS cells derive in the majority of cases from B cells, they display a dramatic deregulation in lineage affiliation, with restricted expression of B cell markers and aberrant expression of multiple markers of other hematopoietic cells. As most of the information about the deregulated phenotype derived from HL cell lines, we isolated 1–30 primary HRS cells by single cell microdissection from affected LNs, performed microarray analyses and compared their expression signatures to those of their putative cells of origin, the germinal center B cells. The trithorax group (TrxG) family member mixed lineage leukemia 5 (MLL5), which was among those genes with a higher expression in HL, was picked as a promising target of research, as recent analyses proved its critical role in stem cell regulation and differentiation of hematopoietic precursors (Liu et al. 2009). This study shows that MLL5 is overexpressed in primary HL and that RNA interference (RNAi) mediated knockdown of MLL5 in several HL cell lines resulted in a significantly decreased proliferation and an increased apoptosis after growth factor withdrawal, while no increase in spontaneous apoptosis could be detected. Moreover, MLL5 down-regulation enhanced responsiveness of HL cell line L1236 towards chemotherapy agent etoposide, possibly mediated through subsequent down-regulation of genes, which might be associated with chemoresistance of L1236, such as the glutathione S-transferase mu 1 (GSTM1). Microarray analyses of MLL5-suppressed L1236 cells showed a decreased expression of genes involved in invasion and metastasis, such as the kinesin family member 18A (KIF18A), which also seems to be overexpressed in HL cell lines as com-

pared to normal hematopoietic cells and other benign tissues. Besides, these same analyses revealed that MLL5 may, to a certain degree, also contribute to expression of B cell-inappropriate genes, e.g. GATA binding protein 3 (GATA3) or enhancer of zeste homolog 2 (EZH2), in HRS cells, as shown for HL cell line HDMYZ. Finally, Western blot analyses revealed a potential role of MLL5 in the epigenetic regulation of gene activation, as global levels of di- and trimethylation of histone 3 at lysine 4 (H3K4me2/me3) as well as global levels of acetlyation of histone 3 at lysine 9 and lysine 14 (H3K9/14Ac) were decreased upon knockdown of MLL5 in several HL cell lines. Taken together, this study demonstrates a capacious role of MLL5 in HL pathogenesis and clears the way for further specific research concerning the contribution of MLL5 in the pathogenesis of this extraordinary disease.

7 Zusammenfassung

Beim Hodgkin Lymphom (HL) handelt es sich um eine maligne Neoplasie des lymphatischen Systems mit einer jährlichen Inzidenz von etwa drei Fällen pro 100.000 Personen, die in den westlichen Industrienationen zwei Krankheitsgipfel zeigt, einen zwischen 15–34 Jahren und einen bei über 60-Jährigen. Als charakteristisch für das Hodgkin Lymphom gelten die vereinzelten großen Tumorzellen, genannt Hodgkin- und Reed-Sternberg (HRS)-Zellen, die typischerweise nur etwa 1% der Zellen in befallenen Lymphknoten darstellen, während der Großteil der Tumormasse aus normalen Immunzellen besteht, die ein entzündliches Begleitinfiltrat bilden. Obwohl die HRS-Zellen in einem Großteil der Fälle von B-Zellen abstammen, zeigen sie eine tiefgreifende phänotypische Deregulation, wobei typische B-Zell-Marker vermindert oder gar nicht mehr exprimiert werden, während eine Vielzahl von Genen, die typisch sind für andere hämatopoietischen Zelllinien, in den HRS-Zellen abnorm überexprimiert werden. Da ein Großteil der Informationen über diesen deregulierten Phänotyp aus Analysen von Zelllinien entstammen, haben wir jeweils 1–30 primäre HRS-Zellen aus befallenen Lymphknoten mittels Laser-Microdissektion isoliert, Microarray-Analysen durchgeführt und schließlich die Genexpressions-Profile dieser Tumorzellen mit denen von Keimzentrums-B-Zellen verglichen, die als Ursprungszellen der HRS-Zellen gelten. Das Mitglied der thrithorax group (TrxG) Familie MLL5 (mixed lineage leukemia 5), welches in den HRS-Zellen eine höhere Genexpression zeigte als in den Keimzentrums-B-Zellen, wurde als interessantes Forschungsobjekt ausgemacht, da neuere Arbeiten zeigten, dass MLL5 maßgeblich an der Stammzellregulation, sowie der Differenzierung und Reifung von hämatopoietischen Vorläuferzellen beteiligt ist (Liu et al. 2009). Diese Arbeit zeigt, dass MLL5 in primären HL Tumorzellen überexprimiert wird und, dass RNA-Interferenz-vermittelte Herunterregulation von MLL5 in verschiedenen HL Zelllinien zu einer signifikant niedrigeren Wachstumsrate und einer erhöhten Apoptoserate nach Wachstumsfaktorenentzug führte, während keine erhöhte spontane Apoptoseneigung

nach Herunterregulation festgestellt werden konnte. Außerdem erhöhte der MLL5 Knockdown in der Zelllinie L1236 das Ansprechen gegenüber dem Chemotherapeutikum Etoposid, eventuell durch nachfolgende Herunterregulation von Genen, die mit einer erhöhten Chemotherapieresistenz von L1236 assoziiert sein könnten, wie zum Beispiel GSTM1 (glutathione S-transferase mu 1). Microarray-Analysen von L1236 MLL5 knockdown Zellen zeigten eine verminderte Expression von Genen, welche die Tumorinvasion und -metastasierung fördern, beispielsweise KIF18A (kinesin family member 18A), welches offensichtlich ebenfalls in HL Zelllinien höher exprimiert wird, als in normalen hämatopoietischen Zellen und anderen gutartigen Geweben. Überdies deuteten die gleichen Auswertungen daraufhin, dass MLL5, jedenfalls bis zu einem gewissen Grad, an der abnormen Expression von B-Zell-untypischen Genen in HRS-Zellen, etwa GATA3 (GATA binding protein 3) oder EZH2 (enhancer of zeste homolog 2), beitragen könnte, wie für die HL Zelllinie HDMYZ gezeigt wurde. Schließlich offenbarten Western Blot Analysen einen möglichen epigenetischen Mechanismus von MLL5, da es nach Knockdown in verschiedenen Zelllinien zu einer Abnahme von aktivierenden Histonmodifiaktionen, nämlich Di- und Trimethylierung am Lysin 4 des Histons 3 (H3K4me2/me3) und Acetylierung am Lysin 9 und 14 des Histons 3 (H3K9/14Ac), kam. Zusammengefasst konnte diese Arbeit eine umfassende Rolle von MLL5 in der Pathogenese des Hodgkin Lymphoms zeigen und ebnet dadurch den Weg für weitere, genauere Untersuchungen, bezüglich der Rolle von MLL5 in der Entwicklung dieser außergewöhnlichen Erkrankung.

List of Tables

List of Figures

References

Ashida N, Senbanerjee S, Kodama S, Foo SY, Coggins M, Spencer JA, Zamiri P, Shen D, Li L, Sciuto T, Dvorak A, Gerszten RE, Lin CP, Karin M, Rosenzweig A. 2011. IKKβ regulates essential functions of the vascular endothelium through kinase-dependent and -independent pathways. Nat Commun, 2:318–318.

Ayton PM, Cleary ML. 2001. Molecular mechanisms of leukemogenesis mediated by MLL fusion proteins. Oncogene, 20(40):5695–5707.

Bai M, Papoudou-Bai A, Kitsoulis P, Horianopoulos N, Kamina S, Agnantis NJ, Kanavaros P. 2005. Cell cycle and apoptosis deregulation in classical Hodgkin lymphomas. In Vivo, 19(2):439–453.

Banerjee D. 2011. Recent Advances in the Pathobiology of Hodgkin's Lymphoma: Potential Impact on Diagnostic, Predictive, and Therapeutic Strategies. Adv Hematol, 2011:439456–439456.

Bargou RC, Leng C, Krappmann D, Emmerich F, Mapara MY, Bommert K, Royer HD, Scheidereit C, Dörken B. 1996. High-level nuclear NF-kappa B and Oct-2 is a common feature of cultured Hodgkin/Reed-Sternberg cells. Blood, 87(10):4340–4347.

Bargou RC, Mapara MY, Zugck C, Daniel PT, Pawlita M, Döhner H, Dörken B. 1993. Characterization of a novel Hodgkin cell line, HD-MyZ, with myelomonocytic features mimicking Hodgkin's disease in severe combined immunodeficient mice. J Exp Med, 177(5):1257–1268.

Benecke H, Lührmann R, Will CL. 2005. The U11/U12 snRNP 65K protein acts as a molecular bridge, binding the U12 snRNA and U11-59K protein. EMBO J, 24(17):3057–3069.

Campo E, Swerdlow SH, Harris NL, Pileri S, Stein H, Jaffe ES. 2011. The 2008 WHO classification of lymphoid neoplasms and beyond: evolving concepts and practical applications. Blood, 117(19):5019–5032.

Carbone A, Gloghini A, Gattei V, Aldinucci D, Degan M, De Paoli P, Zagonel V, Pinto A. 1995. Expression of functional CD40 antigen on Reed-Sternberg cells and Hodgkin's disease cell lines. Blood, 85(3):780–789.

Cartwright RA, Watkins G. 2004. Epidemiology of Hodgkin's disease: a review. Hematol Oncol, 22(1):11–26.

Chandran UR, Ma C, Dhir R, Bisceglia M, Lyons-Weiler M, Liang W, Michalopoulos G, Becich M, Monzon FA. 2007. Gene expression profiles of prostate cancer reveal involvement of multiple molecular pathways in the metastatic process. BMC Cancer, 7:64–64.

Cheng F, Liu J, Teh C, Chong SW, Korzh V, Jiang YJ, Deng LW. 2011. Camptothecin-induced downregulation of MLL5 contributes to the activation of tumor suppressor p53. Oncogene, 30(33):3599–3611.

Cheng F, Liu J, Zhou SH, Wang XN, Chew JF, Deng LW. 2008. RNA interference against mixed lineage leukemia 5 resulted in cell cycle arrest. Int J Biochem Cell Biol, 40(11):2472–2481.

Cheng X, Blumenthal RM. 2008. Mammalian DNA methyltransferases: a structural perspective. Structure, 16(3):341–350.

Chiu A, Xu W, He B, Dillon SR, Gross JA, Sievers E, Qiao X, Santini P, Hyjek E, Lee JW, Cesarman E, Chadburn A, Knowles DM, Cerutti A. 2007. Hodgkin lymphoma cells express TACI and BCMA receptors and generate survival and proliferation signals in response to BAFF and APRIL. Blood, 109(2):729–739.

Claviez A, Canals C, Dierickx D, Stein J, Badell I, Pession A, Mackinnon S, Slavin S, Dalle JH, Chacón MJ, Sarhan M, Wynn RF, Suttorp M, Dini G, Sureda A, Schmitz N, Lymphoma and Pediatric Diseases Working Parties. 2009. Allogeneic hematopoietic stem cell transplantation in children and adolescents with recurrent and refractory Hodgkin lymphoma: an analysis of the European Group for Blood and Marrow Transplantation. Blood, 114(10):2060–2067.

Deans AJ, Simpson KJ, Trivett MK, Brown MA, McArthur GA. 2004. Brca1 inactivation induces p27(Kip1)-dependent cell cycle arrest and delayed development in the mouse mammary gland. Oncogene, 23(36):6136–6145.

Deng LW, Chiu I, Strominger JL. 2004. MLL 5 protein forms intranuclear foci, and overexpression inhibits cell cycle progression. Proc Natl Acad Sci U S A, 101(3):757–762.

Diehl V. 2007. Hodgkin's disease–from pathology specimen to cure. N Engl J Med, 357(19):1968–1971.

Drexler HG. 1992. Recent results on the biology of Hodgkin and Reed-Sternberg cells. I. Biopsy material. Leuk Lymphoma, 8(4-5):283–313.

Dukers DF, van Galen JC, Giroth C, Jansen P, Sewalt RG, Otte AP, Kluin-Nelemans HC, Meijer CJ, Raaphorst FM. 2004. Unique polycomb gene expression pattern in Hodgkin's lymphoma and Hodgkin's lymphoma-derived cell lines. Am J Pathol, 164(3):873–881.

Dürkop H, Hirsch B, Hahn C, Stein H. 2006. cIAP2 is highly expressed in Hodgkin-Reed-Sternberg cells and inhibits apoptosis by interfering with constitutively active caspase-3. J Mol Med (Berl), 84(2):132–141.

Ehlers A, Oker E, Bentink S, Lenze D, Stein H, Hummel M. 2008. Histone acetylation and DNA demethylation of B cells result in a Hodgkin-like phenotype. Leukemia, 22(4):835–841.

Emerling BM, Bonifas J, Kratz CP, Donovan S, Taylor BR, Green ED, Le Beau MM, Shannon KM. 2002. MLL5, a homolog of Drosophila trithorax located within a segment of chromosome band 7q22 implicated in myeloid leukemia. Oncogene, 21(31):4849–4854.

Emmerich F, Meiser M, Hummel M, Demel G, Foss HD, Jundt F, Mathas S, Krappmann D, Scheidereit C, Stein H, Dörken B. 1999. Overexpression of I kappa B alpha without inhibition of NF-kappaB activity and mutations in the I kappa B alpha gene in Reed-Sternberg cells. Blood, 94(9):3129–3134.

Evens AM, Hutchings M, Diehl V. 2008. Treatment of Hodgkin lymphoma: the past, present, and future. Nat Clin Pract Oncol, 5(9):543–556.

Feuerborn A, Möritz C, Von Bonin F, Dobbelstein M, Trümper L, Stürzenhofecker B, Kube D. 2006. Dysfunctional p53 deletion mutants in cell lines derived from Hodgkin's lymphoma. Leuk Lymphoma, 47(9):1932–1940.

Fujiki R, Chikanishi T, Hashiba W, Ito H, Takada I, Roeder RG, Kitagawa H, Kato S. 2009. GlcNAcylation of a histone methyltransferase in retinoic-acid-induced granulopoiesis. Nature, 459(7245):455–459.

Fury W, Batliwalla F, Gregersen PK, Li W. 2006. Overlapping probabilities of top ranking gene lists, hypergeometric distribution, and stringency of gene selection criterion. Conf Proc IEEE Eng Med Biol Soc, 1:5531–5534.

Ghosh S, May MJ, Kopp EB. 1998. NF-kappa B and Rel proteins: evolutionarily conserved mediators of immune responses. Annu Rev Immunol, 16:225–260.

Gore SD, Baylin S, Sugar E, Carraway H, Miller CB, Carducci M, Grever M, Galm O, Dauses T, Karp JE, Rudek MA, Zhao M, Smith BD, Manning J, Jiemjit A, Dover G, Mays A, Zwiebel J, Murgo A, Weng LJ, Herman JG. 2006. Combined DNA methyltransferase and histone deacetylase inhibition in the treatment of myeloid neoplasms. Cancer Res, 66(12):6361–6369.

Heuser M, Yap DB, Leung M, de Algara TR, Tafech A, McKinney S, Dixon J, Thresher R, Colledge B, Carlton M, Humphries RK, Aparicio SA. 2009. Loss of MLL5 results in pleiotropic hematopoietic defects, reduced neutrophil immune function, and extreme sensitivity to DNA demethylation. Blood, 113(7):1432–1443.

Hu JL, Zhou BO, Zhang RR, Zhang KL, Zhou JQ, Xu GL. 2009. The N-terminus of histone H3 is required for de novo DNA methylation in chromatin. Proc Natl Acad Sci U S A, 106(52):22187–22192.

Huang PH, Chen CH, Chou CC, Sargeant AM, Kulp SK, Teng CM, Byrd JC, Chen CS. 2011. Histone deacetylase inhibitors stimulate histone H3 lysine 4 methylation in part via transcriptional repression of histone H3 lysine 4 demethylases. Mol Pharmacol, 79(1):197–206.

Jacobson S, Pillus L. 1999. Modifying chromatin and concepts of cancer. Curr Opin Genet Dev, 9(2):175–184.

Janz M, Stühmer T, Vassilev LT, Bargou RC. 2007. Pharmacologic activation of p53-dependent and p53-independent apoptotic pathways in Hodgkin/Reed-Sternberg cells. Leukemia, 21(4):772–779.

Joos S, Küpper M, Ohl S, von Bonin F, Mechtersheimer G, Bentz M, Marynen P, Möller P, Pfreundschuh M, Trümper L, Lichter P. 2000. Genomic imbalances including amplification of the tyrosine kinase gene JAK2 in CD30+ Hodgkin cells. Cancer Res, 60(3):549–552.

Kanzler H, Küppers R, Hansmann ML, Rajewsky K. 1996. Hodgkin and Reed-Sternberg cells in Hodgkin's disease represent the outgrowth of a dominant tumor clone derived from (crippled) germinal center B cells. J Exp Med, 184(4):1495–1505.

Kapp U, Yeh WC, Patterson B, Elia AJ, Kägi D, Ho A, Hessel A, Tipsword M, Williams A, Mirtsos C, Itie A, Moyle M, Mak TW. 1999. Interleukin 13 is secreted by and stimulates the growth of Hodgkin and Reed-Sternberg cells. J Exp Med, 189(12):1939–1946.

Karube K, Ohshima K, Suzumiya J, Kawano R, Kikuchi M, Harada M. 2006. Gene expression profile of cytokines and chemokines in microdissected primary Hodgkin and Reed-Sternberg (HRS) cells: high expression of interleukin-11 receptor alpha. Ann Oncol, 17(1):110–116.

Kato M, Sanada M, Kato I, Sato Y, Takita J, Takeuchi K, Niwa A, Chen Y, Nakazaki K, Nomoto J, Asakura Y, Muto S, Tamura A, Iio M, Akatsuka Y, Hayashi Y, Mori H, Igarashi T, Kurokawa M, Chiba S, Mori S, Ishikawa Y, Okamoto K, Tobinai K, Nakagama H, Nakahata T, Yoshino T, Kobayashi Y, Ogawa S. 2009. Frequent inactivation of A20 in B-cell lymphomas. Nature, 459(7247):712–716.

Kleer CG, Cao Q, Varambally S, Shen R, Ota I, Tomlins SA, Ghosh D, Sewalt RG, Otte AP, Hayes DF, Sabel MS, Livant D, Weiss SJ, Rubin MA, Chinnaiyan AM. 2003. EZH2 is a marker of aggressive breast cancer and promotes neoplastic transformation of breast epithelial cells. Proc Natl Acad Sci U S A, 100(20):11606–11611.

Klein CA, Seidl S, Petat-Dutter K, Offner S, Geigl JB, Schmidt-Kittler O, Wendler N, Passlick B, Huber RM, Schlimok G, Baeuerle PA, Riethmüller G. 2002. Combined

transcriptome and genome analysis of single micrometastatic cells. Nat Biotechnol, 20(4):387–392.

Küppers R. 2009. The biology of Hodgkin's lymphoma. Nat Rev Cancer, 9(1):15–27.

Küppers R, Rajewsky K, Zhao M, Simons G, Laumann R, Fischer R, Hansmann ML. 1994. Hodgkin disease: Hodgkin and Reed-Sternberg cells picked from histological sections show clonal immunoglobulin gene rearrangements and appear to be derived from B cells at various stages of development. Proc Natl Acad Sci U S A, 91(23):10962–10966.

Lamprecht B, Kreher S, Anagnostopoulos I, Jöhrens K, Monteleone G, Jundt F, Stein H, Janz M, Dörken B, Mathas S. 2008. Aberrant expression of the Th2 cytokine IL-21 in Hodgkin lymphoma cells regulates STAT3 signaling and attracts Treg cells via regulation of MIP-3alpha. Blood, 112(8):3339–3347.

Latham JA, Dent SY. 2007. Cross-regulation of histone modifications. Nat Struct Mol Biol, 14(11):1017–1024.

Leung C, Lingbeek M, Shakhova O, Liu J, Tanger E, Saremaslani P, Van Lohuizen M, Marino S. 2004. Bmi1 is essential for cerebellar development and is overexpressed in human medulloblastomas. Nature, 428(6980):337–341.

Liu H, Westergard TD, Hsieh JJ. 2009. MLL5 governs hematopoiesis: a step closer. Blood, 113(7):1395–1396.

Liu J, Wang XN, Cheng F, Liou YC, Deng LW. 2010. Phosphorylation of mixed lineage leukemia 5 by CDC2 affects its cellular distribution and is required for mitotic entry. J Biol Chem, 285(27):20904–20914.

Lu C, Shi Y, Wang Z, Song Z, Zhu M, Cai Q, Chen T. 2008. Serum starvation induces H2AX phosphorylation to regulate apoptosis via p38 MAPK pathway. FEBS Lett, 582(18):2703–2708.

Lundberg AS, Weinberg RA. 1998. Functional inactivation of the retinoblastoma protein requires sequential modification by at least two distinct cyclin-cdk complexes. Mol Cell Biol, 18(2):753–761.

Ma Y, Visser L, Roelofsen H, de Vries M, Diepstra A, van Imhoff G, van der Wal T, Luinge M, Alvarez-Llamas G, Vos H, Poppema S, Vonk R, van den Berg A. 2008. Proteomics analysis of Hodgkin lymphoma: identification of new players involved in the cross-talk between HRS cells and infiltrating lymphocytes. Blood, 111(4):2339–2346.

MacLachlan TK, Somasundaram K, Sgagias M, Shifman Y, Muschel RJ, Cowan KH, El-Deiry WS. 2000. BRCA1 effects on the cell cycle and the DNA damage response are linked to altered gene expression. J Biol Chem, 275(4):2777–2785.

Madan V, Madan B, Brykczynska U, Zilbermann F, Hogeveen K, Döhner K, Döhner H, Weber O, Blum C, Rodewald HR, Sassone-Corsi P, Peters AH, Fehling HJ. 2009. Impaired function of primitive hematopoietic cells in mice lacking the Mixed-Lineage-Leukemia homolog MLL5. Blood, 113(7):1444–1454.

Marinova Z, Leng Y, Leeds P, Chuang DM. 2011. Histone deacetylase inhibition alters histone methylation associated with heat shock protein 70 promoter modifications in astrocytes and neurons. Neuropharmacology, 60(7-8):1109–1115.

Marshall NA, Christie LE, Munro LR, Culligan DJ, Johnston PW, Barker RN, Vickers MA. 2004. Immunosuppressive regulatory T cells are abundant in the reactive lymphocytes of Hodgkin lymphoma. Blood, 103(5):1755–1762.

Mathas S, Janz M, Hummel F, Hummel M, Wollert-Wulf B, Lusatis S, Anagnostopoulos I, Lietz A, Sigvardsson M, Jundt F, Jöhrens K, Bommert K, Stein H, Dörken B. 2006. Intrinsic inhibition of transcription factor E2A by HLH proteins ABF-1 and Id2 mediates reprogramming of neoplastic B cells in Hodgkin lymphoma. Nat Immunol, 7(2):207–215.

Mauz-Körholz C, Hasenclever D, Dörffel W, Ruschke K, Pelz T, Voigt A, Stiefel M, Winkler M, Vilser C, Dieckmann K, Karlén J, Bergsträsser E, Fosså A, Mann G, Hummel M, Klapper W, Stein H, Vordermark D, Kluge R, Körholz D. 2010. Procarbazine-free OEPA-COPDAC chemotherapy in boys and standard OPPA-COPP in girls have comparable effectiveness in pediatric Hodgkin's lymphoma: the GPOH-HD-2002 study. J Clin Oncol, 28(23):3680–3686.

Mayr MI, Hümmer S, Bormann J, Grüner T, Adio S, Woehlke G, Mayer TU. 2007. The human kinesin Kif18A is a motile microtubule depolymerase essential for chromosome congression. Curr Biol, 17(6):488–498.

Mellor J. 2006. It takes a PHD to read the histone code. Cell, 126(1):22–24.

Mills AA. 2010. Throwing the cancer switch: reciprocal roles of polycomb and trithorax proteins. Nat Rev Cancer, 10(10):669–682.

Ming L, Sakaida T, Yue W, Jha A, Zhang L, Yu J. 2008. Sp1 and p73 activate PUMA following serum starvation. Carcinogenesis, 29(10):1878–1884.

Miranda TB, Cortez CC, Yoo CB, Liang G, Abe M, Kelly TK, Marquez VE, Jones PA. 2009. DZNep is a global histone methylation inhibitor that reactivates developmental genes not silenced by DNA methylation. Mol Cancer Ther, 8(6):1579–1588.

Montesinos-Rongen M, Roers A, Küppers R, Rajewsky K, Hansmann ML. 1999. Mutation of the p53 gene is not a typical feature of Hodgkin and Reed-Sternberg cells in Hodgkin's disease. Blood, 94(5):1755–1760.

Murray PJ. 2007. The JAK-STAT signaling pathway: input and output integration. J Immunol, 178(5):2623–2629.

Müschen M, Rajewsky K, Bräuninger A, Baur AS, Oudejans JJ, Roers A, Hansmann ML, Küppers R. 2000. Rare occurrence of classical Hodgkin's disease as a T cell lymphoma. J Exp Med, 191(2):387–394.

Nagahara M, Nishida N, Iwatsuki M, Ishimaru S, Mimori K, Tanaka F, Nakagawa T, Sato T, Sugihara K, Hoon DS, Mori M. 2011. Kinesin 18A expression: Clinical relevance to colorectal cancer progression. Int J Cancer, 129(11):2543–2552.

Nagel S, Scherr M, Quentmeier H, Kaufmann M, Zaborski M, Drexler HG, MacLeod RA. 2005. HLXB9 activates IL6 in Hodgkin lymphoma cell lines and is regulated by PI3K signalling involving E2F3. Leukemia, 19(5):841–846.

Nakamura T, Mori T, Tada S, Krajewski W, Rozovskaia T, Wassell R, Dubois G, Mazo A, Croce CM, Canaani E. 2002. ALL-1 is a histone methyltransferase that assembles a supercomplex of proteins involved in transcriptional regulation. Mol Cell, 10(5):1119–1128.

Ono M, Scott MS, Yamada K, Avolio F, Barton GJ, Lamond AI. 2011. Identification of human miRNA precursors that resemble box C/D snoRNAs. Nucleic Acids Res, 39(9):3879–3891.

Ooi SK, Qiu C, Bernstein E, Li K, Jia D, Yang Z, Erdjument-Bromage H, Tempst P, Lin SP, Allis CD, Cheng X, Bestor TH. 2007. DNMT3L connects unmethylated lysine 4 of histone H3 to de novo methylation of DNA. Nature, 448(7154):714–717.

Pasman PC, Tiebosch A, Erdkamp FL, Vrints LW, Breed WP, Schouten HC. 1994. P53 as a marker of the malignant cell in Hodgkin's disease. Ann Oncol, 5 Suppl 1:89–91.

Ziemin-van der Poel S, McCabe NR, Gill HJ, Espinosa R, Patel Y, Harden A, Rubinelli P, Smith SD, LeBeau MM, Rowley JD. 1991. Identification of a gene, MLL, that spans the breakpoint in 11q23 translocations associated with human leukemias. Proc Natl Acad Sci U S A, 88(23):10735–10739.

Prince HM, Bishton MJ, Harrison SJ. 2009. Clinical studies of histone deacetylase inhibitors. Clin Cancer Res, 15(12):3958–3969.

Raaphorst FM, van Kemenade FJ, Blokzijl T, Fieret E, Hamer KM, Satijn DP, Otte AP, Meijer CJ. 2000. Coexpression of BMI-1 and EZH2 polycomb group genes in Reed-Sternberg cells of Hodgkin's disease. Am J Pathol, 157(3):709–715.

Re D, Müschen M, Ahmadi T, Wickenhauser C, Staratschek-Jox A, Holtick U, Diehl V, Wolf J. 2001. Oct-2 and Bob-1 deficiency in Hodgkin and Reed Sternberg cells. Cancer Res, 61(5):2080–2084.

Reynolds GM, Billingham LJ, Gray LJ, Flavell JR, Najafipour S, Crocker J, Nelson P, Young LS, Murray PG. 2002. Interleukin 6 expression by Hodgkin/Reed-Sternberg cells is associated with the presence of 'B' symptoms and failure to achieve complete remission in patients with advanced Hodgkin's disease. Br J Haematol, 118(1):195–201.

Richter GH, Plehm S, Fasan A, Rössler S, Unland R, Bennani-Baiti IM, Hotfilder M, Löwel D, von Luettichau I, Mossbrugger I, Quintanilla-Martinez L, Kovar H, Staege MS, Müller-Tidow C, Burdach S. 2009. EZH2 is a mediator of EWS/FLI1

driven tumor growth and metastasis blocking endothelial and neuro-ectodermal differentiation. Proc Natl Acad Sci U S A, 106(13):5324–5329.

Righetti SC, Perego P, Carenini N, Corna E, Dal Bo L, Cedrola S, La Porta CA, Zunino F. 2006. Molecular alterations of cells resistant to platinum drugs: role of PKCalpha. Biochim Biophys Acta, 1763(1):93–100.

Salgado-Garrido J, Bragado-Nilsson E, Kandels-Lewis S, Séraphin B. 1999. Sm and Sm-like proteins assemble in two related complexes of deep evolutionary origin. EMBO J, 18(12):3451–3462.

Schmitz R, Stanelle J, Hansmann ML, Küppers R. 2009. Pathogenesis of classical and lymphocyte-predominant Hodgkin lymphoma. Annu Rev Pathol, 4:151–174.

Schwering I, Bräuninger A, Klein U, Jungnickel B, Tinguely M, Diehl V, Hansmann ML, Dalla-Favera R, Rajewsky K, Küppers R. 2003. Loss of the B-lineage-specific gene expression program in Hodgkin and Reed-Sternberg cells of Hodgkin lymphoma. Blood, 101(4):1505–1512.

Sebastian S, Sreenivas P, Sambasivan R, Cheedipudi S, Kandalla P, Pavlath GK, Dhawan J. 2009. MLL5, a trithorax homolog, indirectly regulates H3K4 methylation, represses cyclin A2 expression, and promotes myogenic differentiation. Proc Natl Acad Sci U S A, 106(12):4719–4724.

Seitz V, Thomas PE, Zimmermann K, Paul U, Ehlers A, Joosten M, Dimitrova L, Lenze D, Sommerfeld A, Oker E, Leser U, Stein H, Hummel M. 2011. Classical Hodgkin's lymphoma shows epigenetic features of abortive plasma cell differentiation. Haematologica, 96(6):863–870.

Skinnider BF, Mak TW. 2002. The role of cytokines in classical Hodgkin lymphoma. Blood, 99(12):4283–4297.

Staege MS, Banning-Eichenseer U, Weissflog G, Volkmer I, Burdach S, Richter G, Mauz-Körholz C, Föll J, Körholz D. 2008. Gene expression profiles of Hodgkin's lymphoma cell lines with different sensitivity to cytotoxic drugs. Exp Hematol, 36(7):886–896.

Stanelle J, Döring C, Hansmann ML, Küppers R. 2010. Mechanisms of aberrant GATA3 expression in classical Hodgkin lymphoma and its consequences for the cytokine profile of Hodgkin and Reed/Sternberg cells. Blood, 116(20):4202–4211.

Steidl C, Connors JM, Gascoyne RD. 2011. Molecular pathogenesis of Hodgkin's lymphoma: increasing evidence of the importance of the microenvironment. J Clin Oncol, 29(14):1812–1826.

Steidl C, Lee T, Shah SP, Farinha P, Han G, Nayar T, Delaney A, Jones SJ, Iqbal J, Weisenburger DD, Bast MA, Rosenwald A, Muller-Hermelink HK, Rimsza LM, Campo E, Delabie J, Braziel RM, Cook JR, Tubbs RR, Jaffe ES, Lenz G, Connors JM, Staudt LM, Chan WC, Gascoyne RD. 2010. Tumor-associated macrophages and survival in classic Hodgkin's lymphoma. N Engl J Med, 362(10):875–885.

Stumpff J, von Dassow G, Wagenbach M, Asbury C, Wordeman L. 2008. The kinesin-8 motor Kif18A suppresses kinetochore movements to control mitotic chromosome alignment. Dev Cell, 14(2):252–262.

Sturn A, Quackenbush J, Trajanoski Z. 2002. Genesis: cluster analysis of microarray data. Bioinformatics, 18(1):207–208.

Ushmorov A, Leithäuser F, Sakk O, Weinhaüsel A, Popov SW, Möller P, Wirth T. 2006. Epigenetic processes play a major role in B-cell-specific gene silencing in classical Hodgkin lymphoma. Blood, 107(6):2493–2500.

Waldman T, Kinzler KW, Vogelstein B. 1995. p21 is necessary for the p53-mediated G1 arrest in human cancer cells. Cancer Res, 55(22):5187–5190.

Wang YW, Qu Y, Li JF, Chen XH, Liu BY, Gu QL, Zhu ZG. 2006. In vitro and in vivo evidence of metallopanstimulin-1 in gastric cancer progression and tumorigenicity. Clin Cancer Res, 12(16):4965–4973.

Weniger MA, Melzner I, Menz CK, Wegener S, Bucur AJ, Dorsch K, Mattfeldt T, Barth TF, Möller P. 2006. Mutations of the tumor suppressor gene SOCS-1 in classical Hodgkin lymphoma are frequent and associated with nuclear phospho-STAT5 accumulation. Oncogene, 25(18):2679–2684.

Winklmeier A, Poser I, Hoek KS, Bosserhoff AK. 2009. Loss of full length CtBP1 expression enhances the invasive potential of human melanoma. BMC Cancer, 9:52–52.

Yu BD, Hanson RD, Hess JL, Horning SE, Korsmeyer SJ. 1998. MLL, a mammalian trithorax-group gene, functions as a transcriptional maintenance factor in morphogenesis. Proc Natl Acad Sci U S A, 95(18):10632–10636.

Yu BD, Hess JL, Horning SE, Brown GA, Korsmeyer SJ. 1995. Altered Hox expression and segmental identity in Mll-mutant mice. Nature, 378(6556):505–508.

Zhang C, Zhu C, Chen H, Li L, Guo L, Jiang W, Lu SH. 2010. Kif18A is involved in human breast carcinogenesis. Carcinogenesis, 31(9):1676–1684.

Zhang Y, Wong J, Klinger M, Tran MT, Shannon KM, Killeen N. 2009. MLL5 contributes to hematopoietic stem cell fitness and homeostasis. Blood, 113(7):1455–1463.

Zhou J, Bi C, Cheong LL, Mahara S, Liu SC, Tay KG, Koh TL, Yu Q, Chng WJ. 2011. The histone methyltransferase inhibitor, DZNep, up-regulates TXNIP, increases ROS production, and targets leukemia cells in AML. Blood, 118(10):2830–2839.

Zhu C, Zhao J, Bibikova M, Leverson JD, Bossy-Wetzel E, Fan JB, Abraham RT, Jiang W. 2005. Functional analysis of human microtubule-based motor proteins, the kinesins and dyneins, in mitosis/cytokinesis using RNA interference. Mol Biol Cell, 16(7):3187–3199.

Acknowledgements

An dieser Stelle möchte ich die Gelegenheit ergreifen, mich bei allen zu bedanken, die zum guten Gelingen dieser Arbeit beigetragen haben.

Mein besonderer Dank gilt Herrn Prof. Dr. Stefan Burdach für die Möglichkeit meine Promotion am Forschungszentrum für krebskranke Kinder der TU München durchzuführen, für die stets wohlwollende und sachkundige Betreuung dieser Arbeit und für die Gelegenheit am *First International Symposium on Childhood, Adolescent and Young Adult Hodgkin Lymphoma* in Arlington, Virginia teilzunehmen. Besonderer Dank gilt außerdem Herrn Dr. Günther Richter für die sehr hilfreiche und fundierte Beratung bei meiner Labortätigkeit, sowie für das entgegengebrachte Vertrauen bei der Durchführung der Experimente.

Herrn Dr. Andreas Mollweide (Klinik und Poliklinik für Kinder- und Jugendmedizin, TU München), Frau Isabell Blochberger, Herrn Matthias Maneck und Herrn Prof. Dr. Christoph Klein (Institut für Pathologie, Universität Regensburg) möchte ich für die essentiellen Vorarbeiten danken, auf denen meine Arbeit maßgeblich aufbaut.

Weiterhin möchte ich mich vor allem bei Stephanie Plehm für die Einarbeitung im Labor, die fürsorgliche Betreuung und den stetigen Rückhalt und Zuspruch bedanken, sowie bei Thomas Grünewald, der mir immer und jederzeit mit Rat und Tat zur Seite stand.

Kristina Hauer, Jens Schmalfuß, Uwe Thiel und insbesondere Colette Zobywalski danke ich dafür, dass sie mir, trotz eigener Belastungen, immer im Labor unter die Arme griffen, wenn dies nötig war.

Nicht zuletzt danke ich vor allem meinen Eltern und meiner Freundin Sarah, ohne deren liebevollen Zuspruch und deren selbstlose Unterstützung diese Arbeit nicht möglich gewesen wäre.